Self-Assembled Multilayered Dielectric Spectral Filters

by

Ashwin Chandran

Thesis submitted to the faculty of
Virginia Polytechnic Institute and State University
in partial fulfillment of the requirements for the degree of

Master of Science
in
Electrical Engineering

APPROVED:

Dr.Richard O. Claus, Chairman
Dr. Roger Stolen
Dr. Wayne A. Scales

September 19, 2001
Blacksburg, Virginia

Keywords: Optical Thin Films, Electro Static Self-Assembly, Dielectric stack filter,
Needle Filters

Self-Assembled Multilayered Dielectric Spectral Filters

Ashwin Chandran

(ABSTRACT)

Thin film optical filters are made by depositing thin films of optical materials on a substrate in such a way as to produce the required optical and mechanical properties. The Electrostatic Self Assembly (ESA) process is accomplished by the alternate adsorption of poly-anionic and poly-cationic molecules on progressive oppositely charged surfaces. This technique offers several advantages such as ease of fabrication, molecular level uniformity, stable multilayer synthesis and avoidance of the need for a vacuum environment. The ESA process offers an excellent choice for manufacturing optical thin film coatings due to its capability to incorporate multiple properties into films at the molecular level and its ability to be a fast and inexpensive process. The ESA process, as a method for manufacturing optical thin film filters has been investigated in detail in this thesis. A specific design was made and analyzed using TFCalc, a commercial thin film design software. Sensitivity analysis detailing the changes in filter response to errors in thickness and refractive index produced by the ESA process were done. These proved that with a high level of quality control, highly reliable and accurate optical thin films can be made by the ESA process.

Table of Contents

Table of Objects

Chapter 1 Introduction

1.1 Optical Filters

Optical spectral filters are of increasing importance in today's world where most of the communication systems are moving towards optical wavelengths. Spectral filters block specific wavelengths or ranges of wavelengths and transmit the rest of the spectrum. These filters could have a variety of applications and depending on the applications the reflectance and transmittance ranges of these filters need to be highly accurate. Spectral filters could be used for wavelength separation for instrumentation or communication systems, protection against damage caused by unwanted wavelengths, for example UV blocking or IR blocking, protection against specific laser lines, as in laser goggles used in laser labs, and other uses.

Thin film optical filters are made by depositing thin films of optical materials on a substrate in such a way as to produce the required optical and mechanical properties. The film thickness is comparable to the wavelength of light and that is why these are called thin film filters.

1.2 Early History of Thin Film Optics

The independent discoveries by Robert Boyle and Robert Hooke of the phenomenon known as "Newton's Rings" could be considered to be the starting point of thin film optics. This phenomenon was due to the interference of light in a single thin film of varying thickness. Due to the lack of understanding of the nature of light, many such thin film effects observed during that period could not be correctly explained. It was only after Thomas Young enunciated the principle of the interference of light in 1801, in a Bakerian lecture to the Royal Society that a satisfactory explanation of these effects could be propounded. The principle of interference of light is the basic principle underlying most of the thin film optical devices and coatings which are being widely used. As Henry Crew said, "The simple but tremendously important fact that two rays of light incident upon a single point can be added together to produce darkness at that point

is, as I see it, the one outstanding discovery which the world owes to Thomas Young [1]."

The work of Augustine Jean Fresnel, which laid a firm foundation for the wave nature of light, is another major land mark in the development of the field of thin film optics [2]. Fresnel's laws governing the amplitude and phase of light reflected and transmitted from a boundary are of major importance in analyzing any thin film optical coating. Maxwell's theory of the electromagnetic nature of light laid another strong stone in the understating of the behavior of thin film effects [3]. Joseph Fraunhofer in 1873 made what are probably the first ever antireflection coatings [4].

In the nineteenth century, a great deal of progress was made in the field of interferometry, and the Fabry-Perot interferometer, described in 1899 [5], became one of the basic structures of thin film filters. Development became much more rapid in the 1930's and it was during this time that the beginnings of modern of thin film optical coatings were made.

1.3 Thin Film Filters

There are two basic approaches to the design of thin film filters. One is to use the property of the deposited material to absorb light of a given wavelength. These are called absorption filters and the wavelength ranges are determined by the molecular properties of the material deposited. Since it is the molecular properties of the materials which determine the properties of the resulting coating, the designer has much less flexibility to work with than for other types of filters considered below. This inflexibility combined with the fact that absorption of radiation over a long period could increase the temperature and cause mechanical damage to the coating, makes these filters practically unattractive. The second method of designing thin film filters is to use the interference effect of light. These are the preferred kind of thin film filters in that they provide the

[1] H.Crew, "Thomas Young's place in the history of the wave theory of light", *J.Opt.Soc.Am*, 20, 3-10(1930).
[2] H.de Senarmont, E.Verdet, L.Fresnel, "Oeuvres complètes d'Augustin Fresnel", 1866-70 (Paris: Impériale).
[3] J.C.Maxwell, "A treatise on electricity and magnetism", Clarendon Press, 1891.
[4] J.von Fraunhofer, "Versuche über die Ursachen des Anlaufens und Mattwerdens des Glases und die Mittel denselben zuvorzukkomen", taken from Joseph von Fraunhofer's *Gessammelte Schriften* (1888).
[5] C.Fabry and A.Perot, "Théorie et applications dune novelle méthode de spectroscopie interférentielle", *Ann.Chim.Phys.*, 16, 115-44(1899).

designer with a wide range of design parameters to produce the required characteristics. The basic type of interference filter consists of a stack of alternate high and low index materials, each one quarter wavelength thick. This quarter wave stack will have high reflectance for a range of wavelengths for which it is designed and the reflectance falls off sharply outside this range. The reflectance of the stack can be made very high just by increasing the number of layers and so it forms a basic building block of many kinds of filters. Optimization approaches towards filter design and the development of highly powerful design software have led to the development of the so called "Needle" filters, where a profile of refractive indices and thickness would look like a line of needles. Chapter 3 deals with thin film interference filters in detail.

1.4 Manufacturing Thin Films

The most important factor in the sudden expansion of thin film optical coatings was the changes that took place in their manufacturing processes. Sputtering and vacuum evaporation were some of the early methods developed for the deposition of films. In the vacuum deposition process the thin films condense from the vapor phase of coating materials and onto the surfaces to be coated which are held at temperatures somewhat lower than the solidification temperature of the films. This process is carried out in an evacuation chamber, to prevent unwanted molecular reactions from taking place. Sputtering consists of bombarding the desired material with ions in a vacuum chamber so that molecules are ejected to collide with and stick to the substrate. In all of these processes, the substrate is held at a temperature much higher than room temperature and requires a vacuum chamber. The control over thickness of the film produced is moderately good, but overall these processes are not very cost effective, especially for large or geometrically shaped substrates.

1.5 Introduction to ESA Processing

The incorporation of molecules into a thin film also can be achieved by molecular self assembly processing, without external intervention. This process produces stable

molecular structures at a local thermodynamic minimum of energy. The driving forces between the molecules are intermolecular attractions typically modeled as classical ionic, hydrogen, van der Waals and covalent bonds. A number of self assembly techniques have been described such as Langmuir - Blodgett (L-B) films and covalently self assembled monolayer processing. A method of developing thin films using the layer by layer adsorption of poly-electrolytes was developed by Decher and co-workers in the early 1990s [6]. This Electrostatic Self Assembly (ESA) process was accomplished by the alternate adsorption of poly-anionic and poly-cationic molecules on progressive oppositely charged surfaces. This technique offers several advantages such as ease of fabrication, molecular level uniformity, stable multilayer synthesis and avoidance of the need for a vacuum environment. This makes ESA thin films highly popular in a variety of applications. The next chapter deals in depth with the ESA process.

1.6 Motivation and Objectives

The real limitation of optical thin film filters and coatings lies in the capability of the manufacturing process to precisely produce thin films of accurate optical constants and thickness, and not in any design issue. The designs of thin film filters and coatings are highly advanced and use various techniques of optimization to obtain the required characteristics. So the real bottleneck in this field is the manufacturing process of thin films.

The ESA process offers an excellent choice for manufacturing optical thin film coatings due to its capability to incorporate multiple properties into films at the molecular level and its ability to be a fast and inexpensive process.

The major objective of this thesis is to design and analyze thin film filters, using the ESA process as the method for making them. The analysis is done using a software called TFCalc, a simulation software used in the analysis of thin films. This thesis work extends the work done by previous researchers in the field of optical thin film filters made by the ESA process. The level of quality control required in the process of ESA for

[6] G.Decher, J.D.Hong and J.Schmitt, "Buildup of ultra thin multi layer films by a self assembly process: II. Consecutively alternating adsorption of anionic and cationic poly electrolytes on charged surfaces", *Thin Solid Films* 210/211, 831(1992).

getting accurate results is studied using some error analysis of certain filter designs. Furthermore, a particular filter design for a specific application is considered.

1.7 Scope of the Thesis

This thesis investigates the ESA process as a method for manufacturing reliable optical thin films. It furthers the work done in this area previously by many researchers in Fiber & Electro-Optic Research Center in Virginia Tech and also work done by groups elsewhere. Most of the work on the ESA process referenced in this thesis has been done by Z.Luo [7] and K.Cooper [8] at the Fiber & Electro-Optic Research Center in Virginia Tech. These works detail how the various variables affect the ESA process and change the nature of the film that is deposited. The reference section at the end of the thesis, contains other works that were referenced. Independent work done during this thesis include sensitivity analysis which determine how the filter performance is affected by variations in thickness and refractive index produced by the ESA process. A hot mirror filter design was done and analyzed. Simulations showing the variations of filter performance with varying angles of incidence and polarization were also done.

[7] Z.Luo, *Linear optical thin films formed by electrostatic self-assembly*, M.S thesis, Electrical Engineering Dept., Virginia Polytechnic Institute & State University, Blacksburg, Virginia, June 2000.

[8] K.Cooper, "Electrostatic self-assembly of linear and nonlinear optical thin films", Ph.D. dissertation, Electrical Engineering Department, Virginia Polytechnic Institute & State University, Blacksburg, Virginia, May 1996.

Chapter 2 ESA Process

2.1 Principle

The basic principle behind Electrostatic Self Assembly is the alternate adsorption of oppositely charged polyions on a charged substrate. A monolayer of polyelectrolyte is assembled on an oppositely charged substrate through ionic bonding, by dipping the substrate in the ionic solution. After rinsing this now coated substrate in ultrapure water to remove the loosely adsorbed molecules, the substrate is then immersed in an oppositely-charged polyelectrolyte solution to adsorb the next molecular monolayer. The resulting coated substrate is again rinsed in ultrapure water. Thus, one bilayer (polycation-polyanion) is synthesized. Repeating this process, we get multilayer structures. A wide variety of molecules, including nonlinear optical chromophores, conducting polymers, biological macro molecules, magnetic materials, dielectrics, and metallic or metallic oxide nanoparticles can be incorporated into the film to achieve specific functionality. This makes ESA practical for a wide variety of applications such as optics, electronics, bio-sensing and surface modification. The composition and structure of each layer can be controlled by appropriately choosing molecules and adjusting the deposition parameters.

The concept of alternate adsorption of oppositely charged polyions began with Iler's demonstration of sequential deposition of negative silica colloids and positive alumina fibrils in 1966 [9]. But it was Decher and his group at the Gutenberg University in Germany who developed this method and fabricated optically transparent multilayer films. UV /vis spectroscopy and small angle X-ray scattering (SAXS) were used to verify the uniform growth of the films [10][11]. Research in this area can be widely grouped into three core groups, one which studies the process itself and tries to comprehend the

---

[9] R.K.Iler, "The adhesion of submicron silica particles on glass", *J.Coll.Inter.Sci*, 38,2, 496-501(1972).

[10] G.Decher, J.D.Hong and J.Schmitt, "Buildup of ultra thin multi layer films by a self assembly process: II. Consecutively alternating adsorption of anionic and cationic poly electrolytes on charged surfaces", *Thin Solid Films* 210/211, 831(1992).

[11] G.Decher, Y.Lvov, J.Schmitt, "Proof of multilayer structural organization in self-assembled poly-cation, poly-anion molecular films", *Thin Solid Films* 244, 772-7 (1994).

variables that control film structure, another which basically studies the material used in the process and tries to incorporate a wider range of molecules for different potential applications, and a third group which studies the possible applications of these films in different fields like optics, electronics and the like. ESA has been used to deposit functional coatings of different types at the Fiber & Electro-Optic Research Center here at Virginia Tech.

2.2 Advantages of ESA process

The ESA process offers the following major advantages over conventional methods of making optical thin films.

- ***Long term stability*** – Since the molecular layers arrange themselves, so as to achieve a thermodynamic minimum, the resulting films are highly stable and their structural ordering does not decay over time.
- ***Synthesis at room temperature and pressure –*** Due to this factor, the films can be adsorbed onto a wide range of solid substrates including semiconductors, plastics, ceramics, metals, organic films etc. without damaging the substrate.
- ***Excellent nanoscale molecular layer uniformity*** – Since the films are made molecular layer by layer, they are extremely uniform and the thickness can be precisely controlled. This permits the fabrication of thin films with extremely low scattering losses.
- ***Compatibility with conventional photolithographic processes*** – Multiple self assembled layers may be patterned using standard methods to create integrated devices.
- ***Capability for high quality multilayer fabrication*** – Uniformity of each layer and elimination of geometrical defects due to conventional covalent bonding based approaches provide an efficient method of preparing high quality multilayers.
- ***Broad range of layer functionality*** – Since alternate anionic and cationic layers are used, materials providing enhanced secondary properties can be

easily incorporated, thus giving excellent control over optical, electronic and mechanical properties of the film.

- ***Low cost manufacturing*** – The process consists of dipping or spraying a charged substrate with oppositely charged polyelectrolyte solutions and rinsing it afterwards. Thus the basic fabrication process is extremely cost effective and can be easily automated.
- ***Long term environmental robustness*** – A defect free molecular order provides high stability and it can be enhanced by incorporating pliable high performance polymers such as polyamides and polymides.
- ***Environmentally friendly*** – Since it is a water based process, it does not involve any volatile organic compounds and the power consumption is also negligible.
- ***Independent of substrate size and topology*** – Unlike Langmuir-Blodgett, sputtering and evaporation processes, substrates of any size or shape maybe coated uniformly on all sides.

2.3 Processing Method

2.3.1 Substrate Processing

The substrates require pre-treatment before applying the multilayer films by ESA process. The common substrates such as quartz, glass and single crystal silicon are first cleaned with a 30:70 mixture of 30% hydrogen peroxide (H_2O_2) and concentrated sulfuric acid (H_2SO_4), called the "piranha solution", at room temperature for one hour. Then the substrate is cleaned using ultra pure water and dried in an oven at 50^0C for several hours. After this treatment, the substrate will be negatively charged. For ITO coated glass substrate, cleaning is done twice in ethanol, using an ultrasonic system. It is then immersed in a 1:1 mixture of ethanol and sulfuric acid at room temperature for one hour and then rinsed in ultra pure water.

2.3.2 Layer-by-layer Processing

Figure 2-1 shows a model for the ESA process. The negatively charged substrate is dipped into a polycationic solution. The cationic molecules are attracted by the anionic substrate and they arrange themselves on the substrate surface to form a molecular monolayer. This is shown in the first part of the figure. The monolayer thus formed has a presumed perfect molecular order, since the molecules are arranged by self assembly.

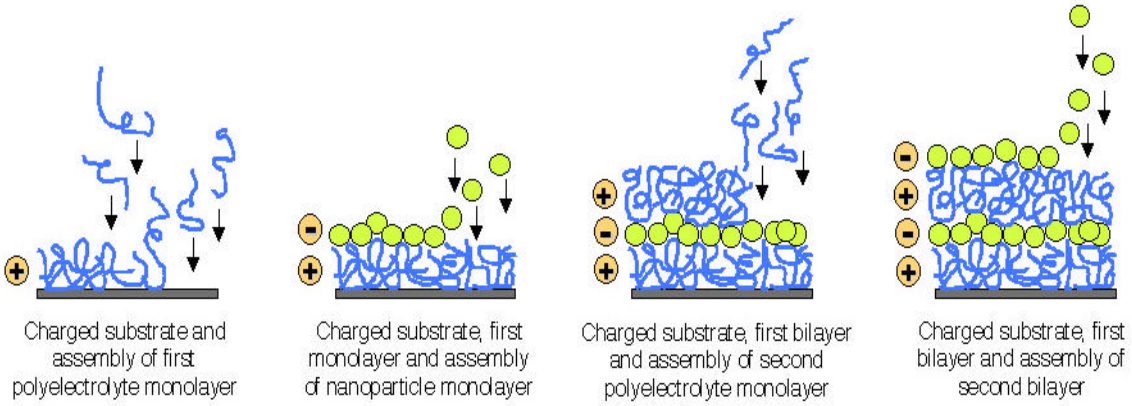

Figure 2-1. The ESA process showing the alternate adsorption of oppositely charged layers.

The first monolayer thus formed is then rinsed with ultrapure water to remove any loosely held particles which may adhere to the layer by means of weak secondary van der Waals forces instead of stronger primary ionic bonds. Next, this is dipped into a polyanionic solution and a negative molecular monolayer is deposited in the same manner. Subsequent bilayer pairs are grown by alternately dipping in oppositely charged aqueous ionic solutions. Individual nanoparticles maybe incorporated into any layer, allowing wide design opportunities.

Solutions of the ionic materials can be made by dissolving the salt forms of the chemical precursor in solvent (typically water) and adjusting the pH.

2.3.3 Drying procedure

In the standard ESA process, the film is not dried and remains wet at all stages. Drying the film to remove the water layer from the film surface affects film characteristics. The drying procedure affects the thickness and optical absorbance of the films. From studies already conducted [12][13] on Poly R-478/PDDA films, dried films (where the film was dried after each monolayer was deposited) showed 20% greater thickness and 15% greater optical absorbance than the un-dried films. This suggests that the un-dried films possess greater inter penetration between the monolayers.

2.3.4 Dipping Time

The dipping time is an important factor in determining the characteristics of the film. Changing the dipping time changes the time available for the ions to arrange themselves and ionically bond to the substrate surface. As the dipping time is increased, the thickness of the layer formed and its optical density also increases, but not in proportion to the time. For example, a 20 minute increase in dipping time, from two to twenty two minutes results in a 20% increase in material thickness. Here the dipping time is increased over 10 times but the thickness change is only 20%. Typically, 1 to 5 minute dipping is used for the layers, depending on the type of materials used.

2.4 Control of Refractive Index

The precise control of the refractive index of each layer is highly necessary for accurate designs of optical thin film filters. The ESA process provides excellent control over refractive indices of the films through a range of available materials. Some of the materials commonly used here, in the Fiber & Electro-Optics Research Center of Virginia Tech are given in Table 2-1.

---

[12] Z.Luo, *Linear optical thin films formed by electrostatic self-assembly*, M.S thesis, Electrical Engineering Dept., Virginia Polytechnic Institute & State University, Blacksburg, Virginia, June 2000.

[13] K.Cooper, "Electrostatic self-assembly of linear and nonlinear optical thin films", Ph.D. dissertation, Electrical Engineering Department, Virginia Polytechnic Institute & State University, Blacksburg, Virginia, May 1996.

Bilayer	Anion	Cation	n at 6328 Å
1	Poly (sodium 4-stvrene-sulfonate)	Polydiallyldimethyl-ammonium chloride	1.539
2	Poly S-119 (Sigma)	PDDA *	1.682
3	PCBS **	PDDA	1.532
4	Direct Red 75 *	PDDA	1.767
5	PSS	ZrO_2	1.567

* from Aldrich
** Poly {1-[4-(3-carboxy-4-hydroxyphenylazo)-benzenesulfonamido]1,2-ethanediyl, sodium salt} (Aldrich)

Table 2-1. Refractive Index Data for 50-Bilayer ESA Films.

ESA films with a single anion/single cation configuration show a linear growth of optical absorbance and film thickness with an increasing number of layers. This suggests that each bilayer contributes equally towards thickness and optical absorbance of the composite film.

Graded index structures can be obtained by combining multiple anions and/or multiple cations in a single film, in varying proportions versus distance. The rule of mixtures effect illustrated in Figure 2-2 is of utmost importance while using multiple ionic mixtures [14]. The figure shows the concept of building up multilayers composed of predetermined patterns of Direct Red 75/PDDA (X) and PSS/PDDA (Y), a mixture of 33% X and 67% Y (XYY) combination. When the percentage of X is varied from 0 to 100%, the optical absorbance of the film increases linearly, indicating that each multilayer is a identical reproducible unit. It is thus possible to grade the index n(x) of the film just by varying the percentage of X. This is the basis of refractive index control for thin films using the ESA process. Figure 2-3 shows the variation of index of a thin film with variation in percentage of X where X is Poly S-119/Platinum Nanoparticle and Y is Poly S-119/PDDA.

[14] K.Cooper, "Electrostatic self-assembly of linear and nonlinear optical thin films", Ph.D. dissertation, Electrical Engineering Department, Virginia Polytechnic Institute & State University, Blacksburg, Virginia, May 1996.

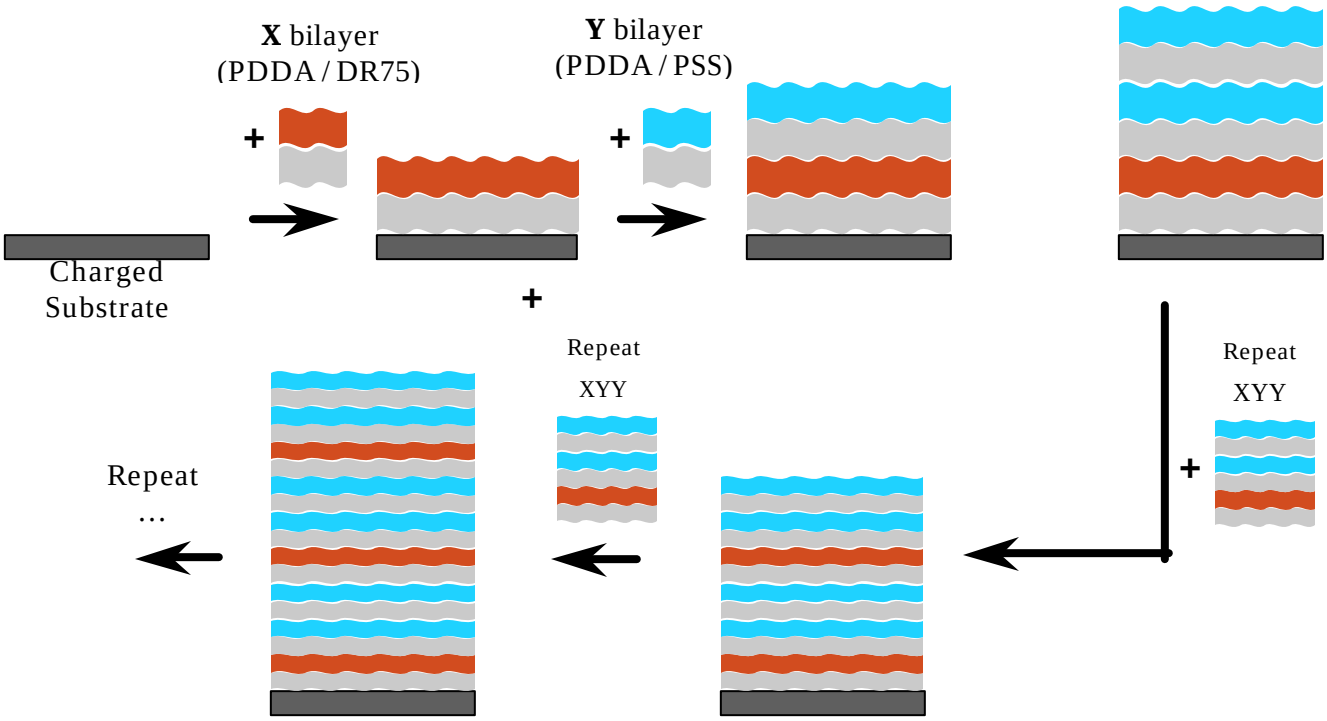

Figure 2-2. Self Assembly of 33:67 mixture (XYY multilayer) ESA film.[15].

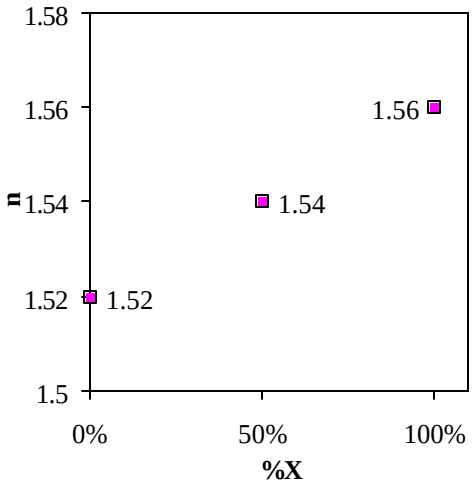

Fig 2-3. Refractive Index vs. Percentage of X (Poly S-119/Platinum Nanoparticle) in 50-Bilayer Films at 6328 A^0; Y=Poly S-119/PDDA Bilayers. [15].

[15] K.Cooper, "Electrostatic self-assembly of linear and nonlinear optical thin films", Ph.D. dissertation, Electrical Engineering Department, Virginia Polytechnic Institute & State University, Blacksburg, Virginia, May 1996.

2.5 Control of thickness

For single anion/single cation ESA films as said before, the thickness increases linearly with number of bilayers [16]. This shows that each layer contributes in equal measure to the whole of the film. This is shown in Figure 2-4.

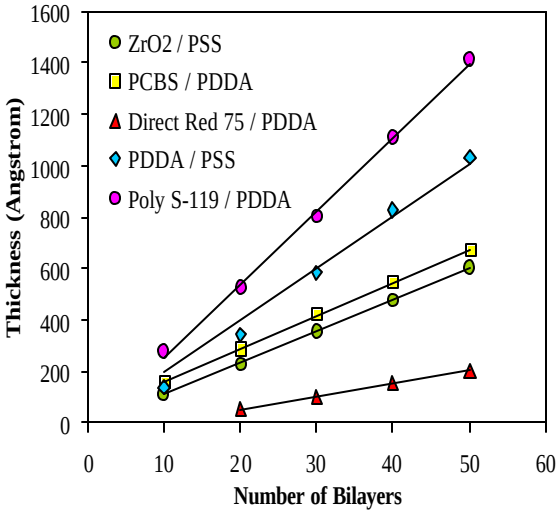

Figure 2-4. Film Thickness with Increasing Numbers of bilayers for Single Anion/ Cation ESA Films [14].

2.6 Automated Vs Hand Dipping

The ESA process is very simple and involves just the dipping of the substrate into the prepared poly ionic solutions for the predetermined time period. So this process can

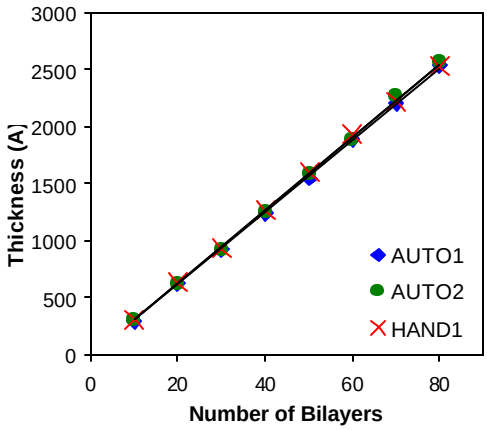

Figure 2-5. Automated Vs Hand Dipping [14].

Figure 2-6. Automated dipping machine.

[16] K.Cooper, "Electrostatic self-assembly of linear and nonlinear optical thin films", Ph.D. dissertation, Electrical Engineering Department, Virginia Polytechnic Institute & State University, Blacksburg, Virginia, May 1996.

be easily automated and the results obtained from hand dipping and automated dipping can be compared to get a good understanding of the reliability. Figure 2-5 shows this [17]. Figure 2-6 shows an automated dipping machine used for ESA process.

2.7 Some examples of ESA coated films

As described earlier, ESA films can be made on substrates of varying sizes and shapes. The following figures shows some examples of ESA films coated on different surfaces [17].

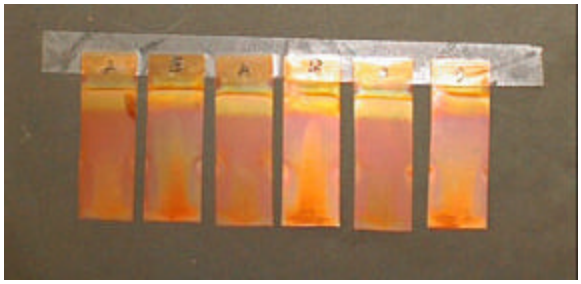

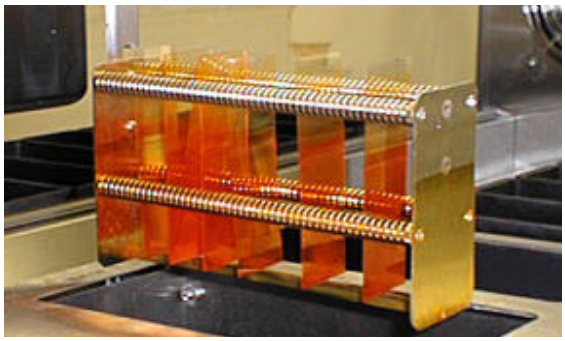

Figure 2-7. Examples of ESA films [3].

2.8 Summary

This chapter dealt in depth with the ESA process. The processing method and control of parameters important for optical thin films were discussed. ESA films for various substrates and the variables controlling the process were introduced and explained in detail.

[17] K.Cooper, "Electrostatic self-assembly of linear and nonlinear optical thin films", Ph.D. dissertation, Electrical Engineering Department, Virginia Polytechnic Institute & State University, Blacksburg, Virginia, May 1996.

Chapter 3. Thin Film Interference Filters

Optical filters can be defined as thickness dependent refractive index systems which modify the properties of a surface to produce the desired optical characteristics. As discussed previously, thin film interference filters are highly popular for applications in a range of fields. These filters can work over a broad range of wavelengths or over a narrow band.

The basic concepts employed in these filters are

i) The amplitude of reflected light at the boundary between two media is given by (1-r) / (1+r) where r is the ratio of refractive indices at the boundary.

ii) There is a phase shift of 180 degrees when reflectance takes place in a medium of lower refractive index than the adjoining medium and zero phase shift if the medium has higher refractive index than adjoining one.

iii) If light is split into two components by reflection at top and bottom surfaces of a thin film, then the beams will recombine in such a way that the resultant amplitude will be the difference of amplitudes of the two components if the relative phase shift is 180 degrees (destructive interference) or the sum of the amplitudes if the relative phase shift is either zero or a multiple of 360 degrees (constructive interference).

Practical application of these thin film filters also requires mechanical properties such as abrasion resistance and hardness.

In the design of a thin film multilayer, we are required to find an arrangement of layers which will produce a specified performance. This is much more difficult than the straightforward calculation of the properties of a given multilayer. There is no analytical solution to the general problem. The normal method of design is to arrive at a possible structure for a filter using some general design techniques and evaluate the performance

of the design, using a design software and refining the design for improved performance. Design softwares capable of making designs from scratch are also available.

3.1 Dielectric Stack Filters

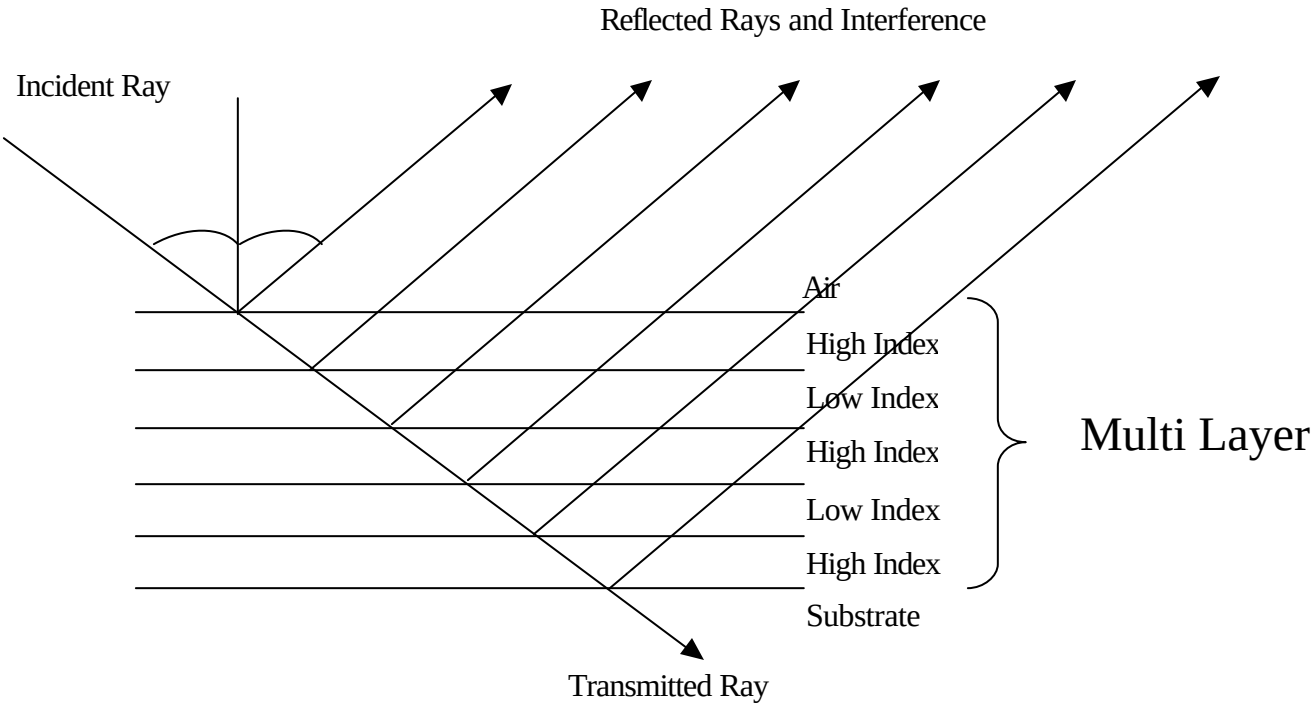

Figure 3-1. Reflection and transmission at layer boundaries.

Figure 3-1 shows a basic type of thin film structure used in filters. It consists of a stack of alternating high and low index dielectric films, all of one quarter wavelength in thickness. Light reflected within the high index layers will not suffer any phase shift due to reflection, whereas the light reflected within the low index film will undergo a 180 degree phase shift as a result of reflection. Since all the film segments are of one quarter wavelength in thickness (90 degree phase thickness) it can be seen that the different components of the incident light produced by the reflection at the different boundaries all arrive in phase at the front surface of the film. These beams combine constructively and the intensity of the reflected beam is very high compared to the transmitted beam. The effective reflectance of the assembly, for a particular wavelength, can be made very high,

just by increasing the number of alternating layers in the stack. The range of wavelengths for which the reflectance remains very high depends on the ratio of refractive indices of the two materials in the stack. Outside this range of wavelengths, the reflectance of the assembly falls abruptly to a very low value. This behavior of the quarter wave stack makes it an ideal building block for many types of filters.

Another approach to filter design is to consider it as a general optimization problem. The variables of optimization will be the thickness of each layer and the refractive index of each layer. It is necessary to optimize the spectral response with respect to thickness and refractive index. Such filters are called "Needle" filters, because a profile of their thickness and refractive indices looks like a line of needles. Different software packages are available which help in the analysis and design of such filters.

3.2 Analysis of a Multilayer Dielectric Stack

Analysis of a multilayer dielectric stack is similar to a boundary value problem. Thin film filters usually consist of a number of boundaries between various homogeneous media and it is the effect which these boundaries will have on the incident wave that we have to calculate.

Considering a single boundary between two homogeneous media of refractive indices n_i and n_t, the reflection and transmission coefficients are given by the Fresnel equations

$$r_s = \frac{n_i \cos\theta_i - n_t \cos\theta_t}{n_i \cos\theta_i + n_t \cos\theta_t} \quad \text{and} \quad t_s = \frac{2n_i \cos\theta_i}{n_i \cos\theta_i + n_t \cos\theta_t}$$

for s polarization and

$$r_p = \frac{n_t \cos\theta_i - n_i \cos\theta_t}{n_i \cos\theta_t + n_t \cos\theta_i} \quad \text{and} \quad t_p = \frac{2n_i \cos\theta_i}{n_i \cos\theta_t + n_t \cos\theta_i},$$

where θ_i and θ_t are the angles made by the incident light with the normal in the incident and transmitted media respectively. At normal incidence, $\theta_i = \theta_t = 0$ and so

$$r_s = -r_p = \frac{n_i - n_t}{n_i + n_t} \quad \text{and } t_s = t_p = \frac{2n_i}{n_i + n_t}.$$

These equations can be used to compute the variation of reflectance of simple boundaries between extended media. These equations have been derived assuming the two media to be non-absorbing, which is usually the case for dielectric films.

3.2.1 Reflectance of a thin film

A simple extension of the above analysis can be used to analyze the reflectance of a thin film.

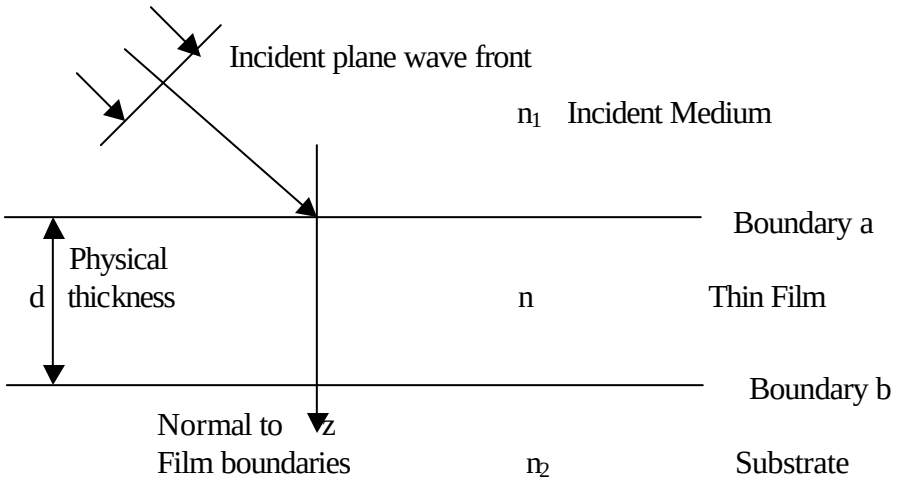

Figure 3-2 Plane wave incident on a thin film

The successive reflections at the multiple interfaces give rise to multiple beams and the summation of these beams determines the properties of the film. The film is said to be 'thin' when the path difference between the different beams is less than the coherence length of light, or in other words, when interference effects can be observed in the beams.

When monochromatic, plane polarized light passes through a thin film, multiple reflections at the interfaces give rise, generally, to two main beams of light advancing in opposite directions. At any point within the medium, these beams will interfere and give rise to a resultant electric field E and a resultant magnetic field H. Considering the light to be incident normally to the surface, the field vectors are parallel to the interfaces. The field vectors E and H at one point are related to fields at another point, E' and H' by the relation

$$\begin{bmatrix} E \\ H \end{bmatrix} = \begin{bmatrix} M_{11} M_{12} \\ M_{21} M_{22} \end{bmatrix} \begin{bmatrix} E' \\ H' \end{bmatrix} \qquad [3\text{-}1]$$

Since the fields are continuous, even at the interface between the two media, the matrix in the equation describes the thin film between the two points in question, without relation to the surrounding media. Matrices of these types were introduced into optics by A. Herpin, and are called Herpin matrices [18]. One important property of Herpin matrices is that their determinant is always 1. The matrix defining the whole thin film between the 'boundary a' and 'boundary b' as shown in Figure 3.2 is given by

$$\begin{bmatrix} \cos\delta & \frac{(i\cdot\sin\delta)}{n} \\ in\cdot\sin\delta & \cos\delta \end{bmatrix}, \qquad [3\text{-}2]$$

where $\delta = 2p*n*d/\lambda$, n is the refractive index of the homogeneous film and d is the physical thickness of the film. For light incident at an angle θ, $\delta = 2p*n*d*\cos\theta/\lambda$.

Therefore, we have

$$\begin{bmatrix} E_a \\ H_a \end{bmatrix} := \begin{bmatrix} \cos\delta & \frac{(i\cdot\sin\delta)}{n} \\ i\cdot n\cdot\sin\delta & \cos\delta \end{bmatrix} \cdot \begin{bmatrix} E_b \\ H_b \end{bmatrix} \qquad [3\text{-}3]$$

where E_a, H_a are the fields at boundary a and E_b, H_b are fields at boundary b. Defining the optical admittance of the thin film to be $Y = H_a/E_a$, we have

$$Y := \frac{n_2\cdot\cos\delta + i\cdot n\cdot\sin\delta}{\cos\delta + i\frac{n_2}{n}\sin\delta} \qquad [3\text{-}4]$$

For a combination of two or more thin films, the resulting matrix is given by the product of the individual matrices of the two films, in the order in which they occur.

[18] A.Herpin, *Compt.rend.* 225, 182 (1947).

3.2.2 The Herpin index

Epstein in 1952 published a paper [19] which dealt with the mathematical equivalence of a symmetrical combination of thin films. Any combination of thin films can be considered to be symmetrical if one half is a mirror image of the other half. A symmetrical three layer film combination of the type *pqp* is widely popular in thin film filter designs. The characteristic matrix of this combination is given by

$$\begin{bmatrix} M_{11} & M_{12} \\ M_{21} & M_{22} \end{bmatrix} = \begin{vmatrix} \cos\delta_p & \frac{(i\cdot\sin\delta_p)}{n_p} \\ in_p\cdot\sin\delta_p & \cos\delta_p \end{vmatrix} \begin{vmatrix} \cos\delta_q & \frac{i\cdot\sin\delta_q}{n_q} \\ in_q\cdot\sin\delta_q & \cos\delta_q \end{vmatrix} \begin{vmatrix} \cos\delta_p & \frac{(i\cdot\sin\delta_p)}{n_p} \\ in_p\cdot\sin\delta_p & \cos\delta_p \end{vmatrix} \quad [3\text{-}5]$$

From which, $M_{11} = \cos 2\delta_p * \cos\delta_q - \frac{1}{2}\left(\frac{n_q}{n_p} + \frac{n_p}{n_q}\right)\sin(2\delta_p)*\sin\delta_q$,

$$M_{12} = \frac{i}{n_p}\left[\sin(2d_p)\cos d_q + \frac{1}{2}\left(\frac{n_q}{n_p}+\frac{n_p}{n_q}\right)\cos(2d_p)\sin d_q + \frac{1}{2}\left(\frac{n_p}{n_q}-\frac{n_q}{n_p}\right)\sin d_q\right],$$

$$M_{21} = in_p\left[\sin(2d_p)\cos d_q + \frac{1}{2}\left(\frac{n_q}{n_p}+\frac{n_p}{n_q}\right)\cos(2d_p)\sin d_q - \frac{1}{2}\left(\frac{n_p}{n_q}-\frac{n_q}{n_p}\right)\sin d_q\right],$$

and $M_{22} = M_{11}$.

Let $M_{11} = \cos\gamma = M_{22}$ and let $M_{12} = i.\sin\gamma/E$, then, since the determinant of the resulting matrix is one, $M_{11}M_{22} - M_{12}M_{21} = 1$, so $M_{21} = i.E.\sin\gamma$.

So the resulting matrix is of the form $\begin{bmatrix} \cos g & \frac{i.\sin g}{E} \\ i.E.\sin g & \cos g \end{bmatrix}$ which is exactly similar to that of the single film matrix. So the symmetrical three layer period *pqp* can be considered to be equivalent to just one film of refractive index E and phase thickness γ.

[19] L.I.Epstein, "The design of optical filters", *J.Opt.Soc.Am.* 42,11 (1952).

So, effective index, $E = +\sqrt{\frac{M_{21}}{M_{12}}}$, and effective phase thickness $\gamma = \arccos(M_{11})$.

These results can be extended to any symmetrical period with any number of layers. The equivalent index, thus obtained, is known as the Herpin index and this forms a very important mathematical tool in the design of thin film coatings. The equivalent single layer representation is not an exact replacement for the symmetrical combination in all physical aspects. It is only a mathematical model for representing the combination of the symmetrical periods. The effect of change of incidence angle cannot be estimated by this method of equivalent layer. Since it is not an exact physical model, the elements of the matrix also depend upon wave number, polarization and angle of incidence of the incident light.

If a multilayer is made up of N identical periods, each of equivalent index E and phase thickness γ then the multilayer will have an equivalent phase thickness of $N\gamma$ and equivalent index of E, which is derived from the relation

$$\begin{bmatrix} \cos g & \frac{i.\sin g}{E} \\ i.E.\sin g & \cos g \end{bmatrix}^N = \begin{bmatrix} \cos(Ng) & \frac{i.\sin(Ng)}{E} \\ i.E.\sin(Ng) & \cos(Ng) \end{bmatrix} \qquad [3\text{-}6]$$

If M_{12} and M_{21} both have equal signs then the effective index, E is real else E is purely imaginary. When E is imaginary, $|\cos\gamma|$ becomes greater than one. The physical significance of this is very important in understanding stop-bands created by a thin film structure. As the number of basic periods increases in a multilayer, the reflectance tends to unity in regions where $|M_{11}| = |M_{22}| > 1$. So an imaginary index and phase thickness represents a stop-band in the spectrum, where the reflectance is 100%. The edges of this stop-band are given by equating $M_{11} = -1$.

The basic quarter wave stack can be represented as $[L/2\ H\ L/2]^N$ or $[H/2\ L\ H/2]^N$ where L is the low index material and H is the high index material. This is exactly like the *pqp* structure analyzed and all the results derived can be applied to this.

3.3 Design Techniques for Thin Film Filters

The design of multilayer filters involves tedious calculations of the reflectance and transmission taking place at each surface of the films in the stack. There are many techniques that are used to make these designs simpler. Some of the commonly used techniques in thin film design are the following:

- **The Vector Method** : This method is usually associated with the design of anti-reflection coatings. Two assumptions are involved, first that the layers are all non-absorbing, and second that the behavior of the multilayer can be understood by considering one reflection of the incident wave at each interface. The errors involved can be significant especially when overall reflectance from the multilayer does exist. The reflection coefficient at each interface is represented by a vector of magnitude $R_r = \frac{n_{r-1} - n_r}{n_{r-1} + n_r}$ and phase $\delta_r = 2pn_r d_r/\lambda$, where n_r is the refractive index of the r^{th} layer and d_r is the thickness of the r^{th} layer. The resultant amplitude coefficient of the stack is given by the vector sum of coefficients for each interface. This sum can be found graphically or analytically.
- **Smith's Method** : Smith in 1958 formulated a method known as the method of effective interfaces for designing multilayer thin film filters [20]. It consists of choosing any layer in the multilayer and then considering multiple reflections within it. The reflection and transmission coefficients at the boundaries of the layer are considered to be the resultant coefficients of the complete structures on either side. This technique can be extended to deal with absorbing layers also. This method provides an insight into the properties of a particular type of filter, but is highly complicated.
- **The Smith Chart** : The Smith chart is a device which is intended to simplify calculations involved in the design of thin film filters. This chart represents circles of constant amplitude coefficient and circles of constant real part and constant imaginary part of the reduced optical admittance. A scale, calibrated

[20] S.D.Smith, "Design of multilayer filters by considering two effective interfaces", *J.Opt.Soc.Am.* 48,43-50 (1958).

in terms of optical thickness is provided around the outside of the chart. This enables the calculation to be very simply carried out by rotating the point corresponding to the amplitude reflection coefficient of the particular layer, around the center of the chart through the appropriate angle.

- **Circle Diagrams** : In this method, the multilayer is considered to be gradually built up layer by layer, immersed all the time in the final incident medium. As each layer increases from zero to its final value, some parameter of the multilayer at that stage, like reflectance or admittance, is calculated and the locus is plotted. The loci for these dielectric layers take the form of a series of circular arcs or even complete circles, each corresponding to a single layer, which are connected at points corresponding to interfaces between different layers.

3.3.1 Optimization Techniques

Any discussion of filter design techniques will be incomplete without detailing the new computer aided analysis and design techniques available. These methods of computer refining consider the problem of multilayer filter design as an optimization problem and this method was first introduced by Baumeister in 1958 [21]. By using this technique it is possible to apply all the powerful tools of modern computation to the design of optical coatings. The basic principle behind this approach is to define a merit function for all coatings and this merit function has to be minimized by the changing of several design variables like the thickness and refractive indices of the individual layers. The optimization of the merit function is a highly complicated task due to the fact that there can be several local minima for the merit function. The optimization process is highly reduced when there is a good starting design. A powerful new technique, known as the "*Needle Optimization Technique*" has been developed for the design and refinement of thin film optical coatings.

[21] P.Baumeister, "Design of multilayer filters by successive approximations", *J.Opt.Soc.Am.* 48,955-958 (1958).

3.3.2 Needle Optimization Technique

The basic idea for the Needle optimization technique was proposed in 1982 and the first computer code that implemented it was developed for use on the Russian BESM-6 mainframe [22]. A thin film filter functions on the basis of interference effects. These effects are determined by the phase and amplitude of reflected light waves. The numerical measure of the correspondence between actual and desired spectral characteristics of the design is provided by the merit function of the coating. The smaller the value of the merit function, the closer the correspondence between target and actual values. When the merit function is optimized with respect to layer thickness, the phase relationship among the reflected waves is changed. If optimization with respect to layer refractive indices is performed then in effect the amplitude of the reflected waves is also being changed. The mathematical optimization process is finished when it becomes impossible to minimize the merit function further. To proceed further with optimization, new layers have to be introduced into the existing multilayer structure. Such insertions are equivalent to changing the refractive index profile of the stack and these variations are referred to as needle variations of the refractive index profile. If the new layers are introduced in the correct places then the interference effect associated with these new layers will improve the correspondence between target and actual values [23].

The essence of the needle optimization process is that its algorithm identifies the proper places, if they exist, to insert new layers that will improve the merit function. The algorithm also identifies which material from a pre-selected group of materials will provide the greatest improvement. There is an analytic algorithm which allows the calculation of the change in the merit function as a function of the refractive index and position of a new layer, without actually inserting the new layer. This is a rather complicated algorithm, but it is extremely efficient.

---

[22] A.V.Tikhonravov, "Synthesis of optical coating using optimality conditions", *Vestn.Mosk.Univ.Fiz.Astronomiya* 23, 91-93(1982).

[23] A.V.Tikhonravov, M.K.Trubetskov, and G.W.DeBell, "Application of the needle optimization technique to the design of optical coatings", *Appl.Opt.* 35,28(1996).

3.4 Types of Filters

Depending on the application and design, there are different types of optical filters. The main types of filters widely used are:

- **Antireflection Coatings** : These were the main objective of much of the early work in thin film optics. Antireflection coatings are required for reducing surface reflections and also to increase transmittance. They can range from a single layer having zero reflectance at one wavelength to a multilayer structure having zero reflectance over a range of wavelengths.
- **High Reflectors and Beam Splitters** : These coatings reflect a major portion of the incident light. Applications usually have the requirement to maximize the specular reflectance, and sometimes also require the absorbance to be extremely low. Multilayer all dielectric reflectors combine maximum reflectance with minimum absorption.
- **Edge Filters** : Edge filters have an abrupt change between a region of rejection and a region of absorption. There are two main kinds of edge filters, long wave pass and short wave pass filters. Long wave pass filters pass the longer wavelengths of the spectrum and block the shorter wavelength part of it, and vice versa for short wave pass filters.
- **Band-pass Filters** : These filters possess a region of transmission bound on either side by regions of rejection. Band pass filters can be of the broad band pass type or narrow band pass type.
- **Minus Filters** : Minus filters eliminate one wavelength band from a spectrum, i.e., they have a narrow region of rejection, bound on either side by regions of transmission.

3.5 Summary

This chapter dealt in detail with optical filters in general and thin film filters in particular. Techniques for analyzing the performance of thin films and popular methods of designing thin film optical coatings were discussed. The different types of filters and their applications were also introduced.

Chapter 4 TFCalc Filter Design Software

4.1 Introduction

TFCalc is a commercial thin film design and analysis software for windows, developed by Software Spectra Inc. The flow diagram in Figure 4-1 shows in general how to use the TFCalc software to design a thin film coating.

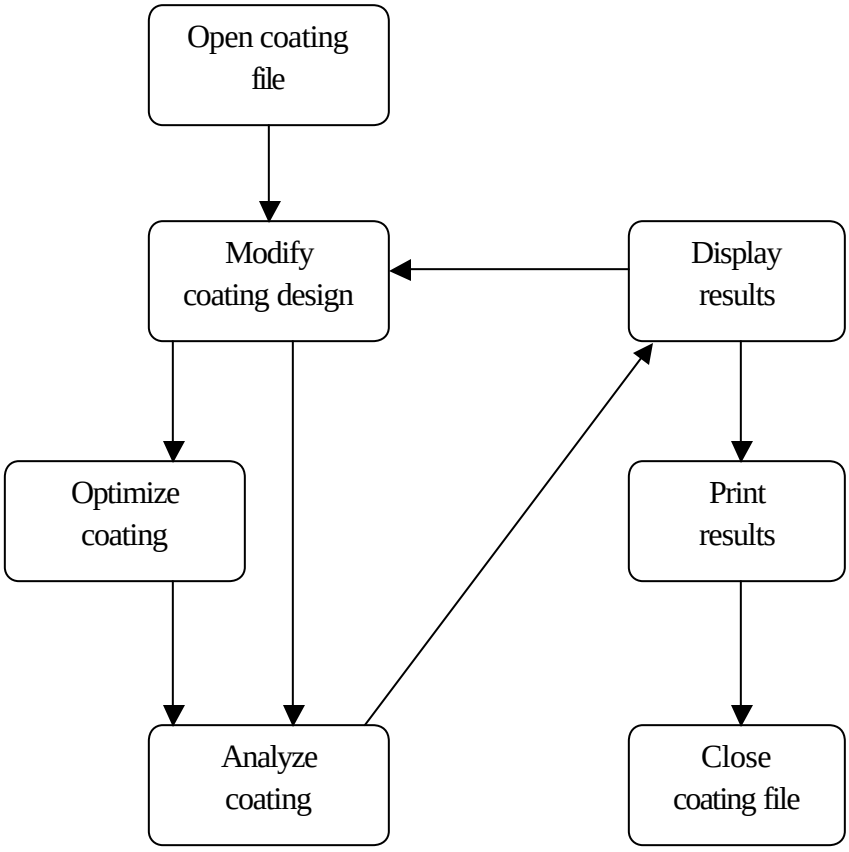

Figure 4-1. Flowchart showing the method of design using TFCalc.

TFCalc is useful for analyzing a pre-designed multilayer structure, as well as for the automatic design to meet specific performance criteria. The process begins by opening a new or existing coating file. The designer then modifies the coating and may optimize or analyze the coating. Now the results can be viewed and printed and finally the coating file is saved and closed for future reference.

4.2 The Model

Figure 4-2 shows the physical system modeled by TFCalc.

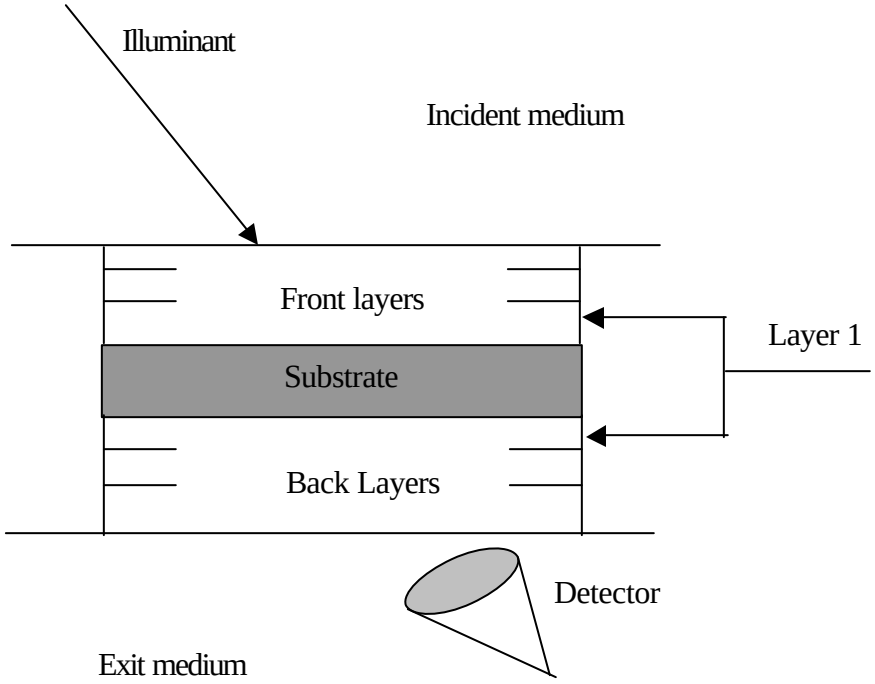

Figure 4-2. Physical system modeled by TFCalc.

The illuminant stored in the illuminant database is given as a table of spectral intensity versus wavelength. The incident angle may vary from 0 to 89.999 degrees. The substrate, incident and exit media are selected from the substrate database. The detector is selected from the detector database and is given as a table of efficiency versus wavelength. The thickness of the substrate can be specified and the incident and exit media can be absorbing materials. The materials making up the front and back layers are selected from the material database. In the version used for the purpose of this thesis work, i.e. version 3.4.3, there is a limit of a total of 5000 layers. The optical properties of substrates and materials are stored as tables or dispersion formulae of complex refractive index (n-ik) versus wavelength. Layer 1 is the layer next to the substrate. New materials or substrates can be added to the existing database.

4.3 Features

TFCalc software can analyze and design multilayer thin film coatings. Some of its features are:

- Reflectance, transmittance, absorptance, optical density, loss, color, luminance, psi, phase shift on reflectance or transmission, and electric field intensity may be computed and plotted.
- The sensitivity of the coating to manufacturing errors may be analyzed. Optimization can be used to minimize the sensitivity. Layer sensitivity can be computed and displayed.
- A coating can be analyzed for a cone of angles and a user defined radiation distribution.
- The coating materials, the substrate, and the exit medium may be dispersive and absorbing. The incident medium may be dispersive. Dispersion formulae can be used to give the index of materials and substrates.
- A coating can have up to 5000 layers, composed of up to 150 different materials.
- The illuminant may be specified . The reflectance and transmittance of a thin film may be stored as an illuminant, so that the output of one filter can be made the input of another. Also blackbody illuminants may be specified.
- Stacks of layers may be entered using a formula, such as (LHL)^p.
- Layers may be arranged in groups, and the groups may be optimized.
- The index (n and k) and thickness of a layer can be optimized.
- Global search may be used to locate the best design, rather than just the local minima.
- Up to 5000 optimization targets can be specified.
- Multiple environments can be used to develop coatings for multiple substrates.
- Needle optimization can add layers to a design automatically.

- Targets may be generated automatically or read from files.
- Equivalent index of a symmetrical stack of layers may be computed.
- A choice of three optimization techniques, Gradient Variable metric, or Simplex, are available.
- Data for unlimited number of illuminants, detectors, material, substrates and distributions may be entered
- Optical monitoring curves may be computed and plotted.
- The minimum, maximum and average values of a parameter like reflectance can be computed for a wide range of wavelengths.
- The results may be saved to text files for processing by other software.

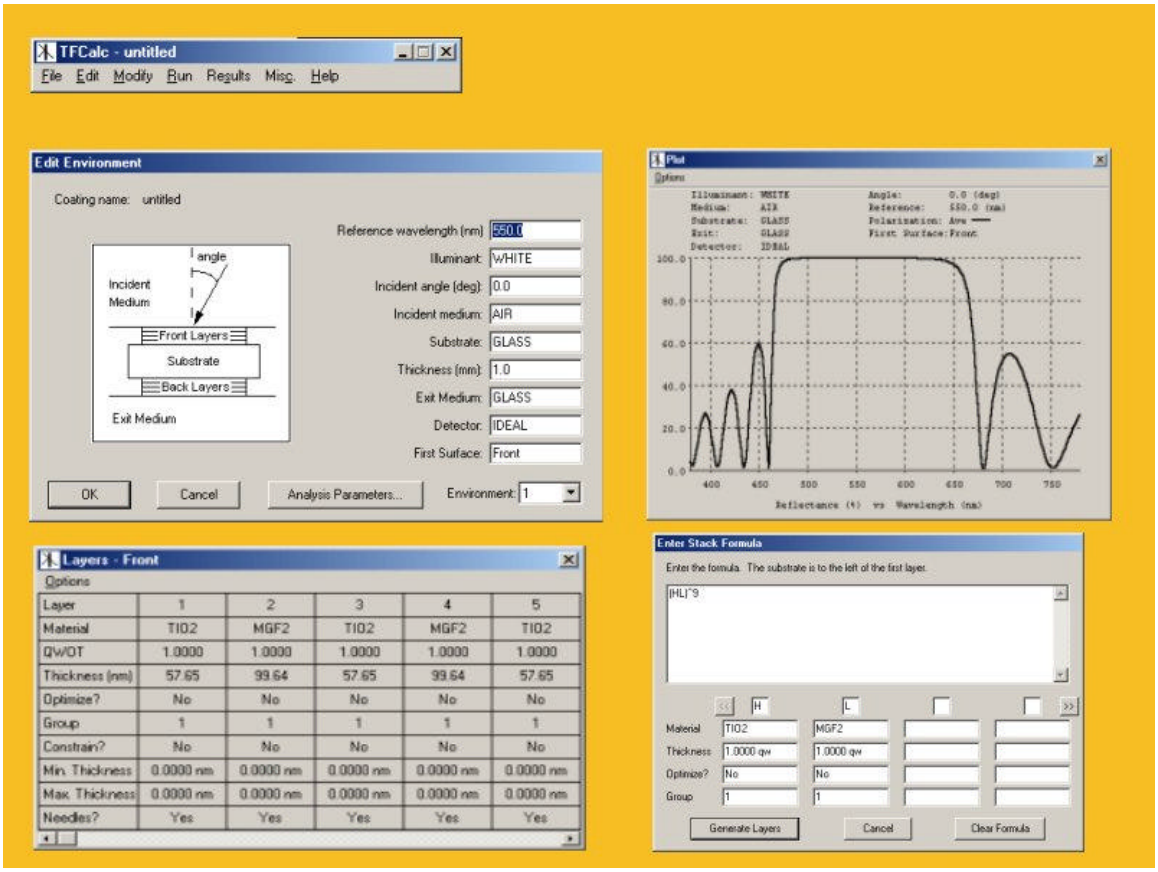

Figure 4-3. Interface of TFCalc.

Figure 4-3 shows some of the windows in the user interface of TFCalc.

4.3.1 Design Optimization

Design optimization is a very powerful feature available to the designer using TFCalc software for designing thin films. A choice of three optimization methods, Gradient, Variable Metric and Simplex, are available. Layers on both sides of the substrate can be optimized simultaneously and up to 1000 optimization targets can be specified. The Optimize Design command in TFCalc tells the program to vary the thickness of the layers or the group factors of the groups and the index of the variable of materials, so that the following merit function is minimized:

$$F = \left(\frac{1}{m} \sum_{j=1}^{m} \left| \frac{I_j D_j C_j - T_j}{N_j Tol_j} \right|^k \right)^{1/k} \qquad [4\text{-}1]$$

where m is the number of targets, k is the power of the method, I is the intensity of the illuminant, D is the efficiency of the detector, T is the desired target value, C is the computed value (of reflectance, transmittance etc. at the target wavelength, angle and polarization), Tol is the tolerance for a target and N is the normalization factor for the target. In most cases, I = D = Tol = 1.0. For continuous targets, the above summation is replaced by a sum of integrals.

The value $\frac{I_j D_j C_j - T_j}{N_j}$ is called the deviation from the target. The normalization factor converts the units to a compatible scale. The normalization factor for reflectance, transmittance, absorptance, and luminance is 1.0, for phase targets, it is 1.8, for density targets it is 0.09 and for color targets it is 0.01. The power of the method, k, can have a very important effect on the result obtained. The program allows for the following values of k: 1, 2, 4, 8, 16, and Max. As the value of k is increased, the larger deviations will be emphasized, forcing the optimization methods to equalize the deviations of the targets. When k is set to Max, the merit function is defined to be the maximum of the deviations: $F = \underset{j}{Max} \left| \frac{I_j D_j C_j - T_j}{N_j Tol_j} \right|$ because this function is not smooth, only the simplex method works when k = Max. Optimization continues till either the maximum

number of iterations is reached, the solution is found or the Quit button is selected. Global search enables the user to locate a global minimum rather than a local minimum.

4.3.2 Sensitivity analysis

Compute sensitivity command provides the designer an option to compute the sensitivity of the design to small manufacturing error. The expected error of thickness or index can be set by the designer. The sensitivity computation selects thickness or indices of layer randomly, analyze the coating design by the Monte Carlo method and records the results. The sensitivity analysis forms an important part of the analysis done in the next chapter to compute the sensitivity of normal designs to errors in the ESA process.

The layer sensitivity function lets the user calculate which layer is most sensitive to manufacturing errors. This is generally used only after a design has been totally optimized. Several other features like computing the electric field intensity and plotting it, analyzing the filter, considering the illumination to be in the form of a cone etc are available in the software.

4.4 Summary

TFCalc which is a commercially available, powerful thin film analysis and design software was introduced and some of its main features were discussed in length in this chapter.

Chapter 5. Error Analysis

The sensitivity of a thin film design to manufacturing errors of the ESA process is analyzed in this chapter using the TFCalc filter design software. Due to several factors errors may occur in thickness of the film and/or index of the film being deposited. Since the index of the film depends on the material being used and less on the ESA process itself, the errors in index produced by the manufacturing process is negligible. So the analysis is mainly done from the point of errors in the thickness of films.

Three quarter wave dielectric stack filter designs without optimization for thickness or index and one dielectric stack filter that has been optimized for thickness of the layers were used to study the sensitivity to errors.

5.1 Designs used for simulations

Three quarter wave stack designs using two materials were considered, keeping the lower index material the same (n = 1.4) for all the three designs. Three designs were used to find how the sensitivity changes when the ratio of the indices between the two materials changes.

From recent and past studies, it has been established that an error of ± 5% is an upper limit to the thickness errors that could occur during the ESA process. Errors as low as ± 0.2% have been reported recently [24]. Based on these facts, error sensitivity for these filter designs were carried out. Three error sensitivity simulations, one with a maximum error of ± 5%, another with an upper bound of ±1% and the last with a maximum error of ±0.2%, all three with the errors distributed randomly (Gaussian distribution is used) among all the layers, are used to compare the sensitivity. In all these three cases, the refractive index is assumed to be error free. One simulation, with a maximum error of ±5% for thickness combined with a ±1% error in refractive index of the materials was also done. The errors in all the cases were worst case scenarios giving the maximum and minimum responses computed using the Monte Carlo method.

---

[24] G.Decher, "Fuzzy nanoassemblies: Toward layered polymeric multicomposites", Science, 277, 1232-1237 (1997).

5.1.1 Design # 1

For the first quarter wave stack design the stack formula of (0.5L H 0.5L)^9 was used, with L being a material of refractive index 1.4 and H being a material of index 1.7. The center wavelength was taken to be 550nm. The basic symmetric period is repeated 9 times. A white illuminant was used and air with n=1.0 was the incident medium and glass with n=1.52 was the substrate and exit medium. The detector is assumed to be ideal and wideband. The design is centered at a wavelength of 550nm. Figure 5-1 shows the simulated reflectance spectra for this design.

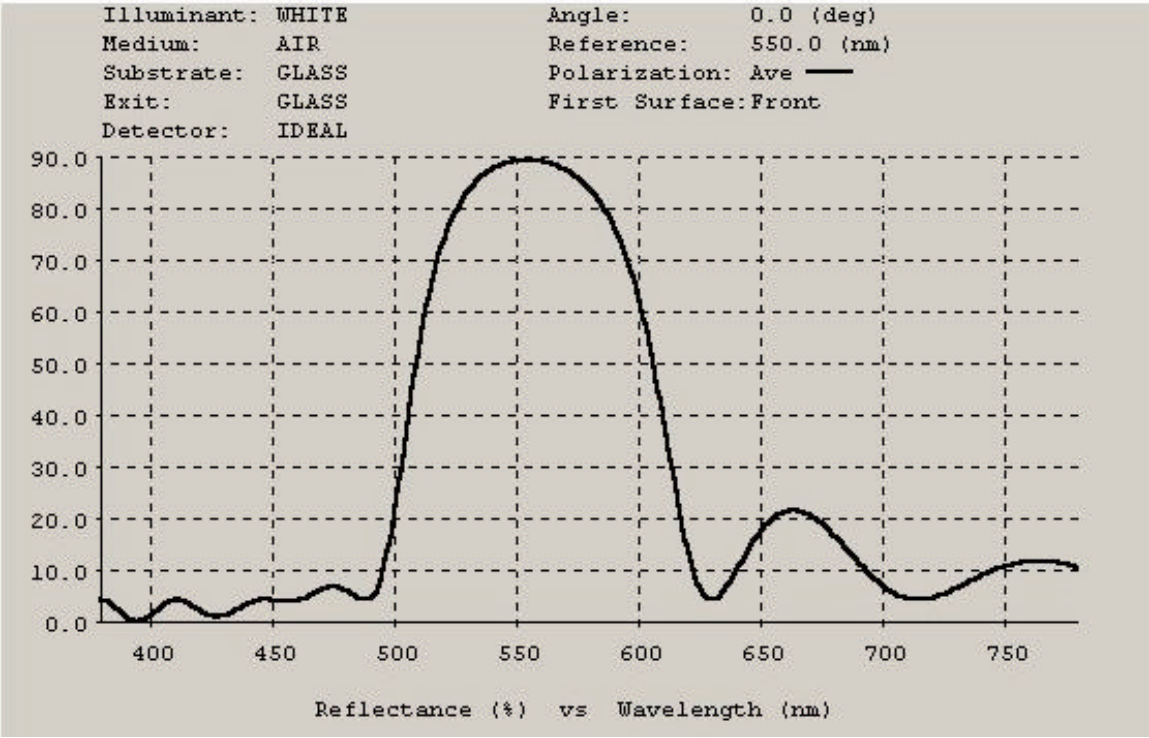

Figure 5-1. simulated reflectance spectra for design #1.

Figure 5.2 shows the simulated reflectance spectra for this design with a ±5% max error distribution in the thickness of the films. The refractive index is assumed to be error free for this case.

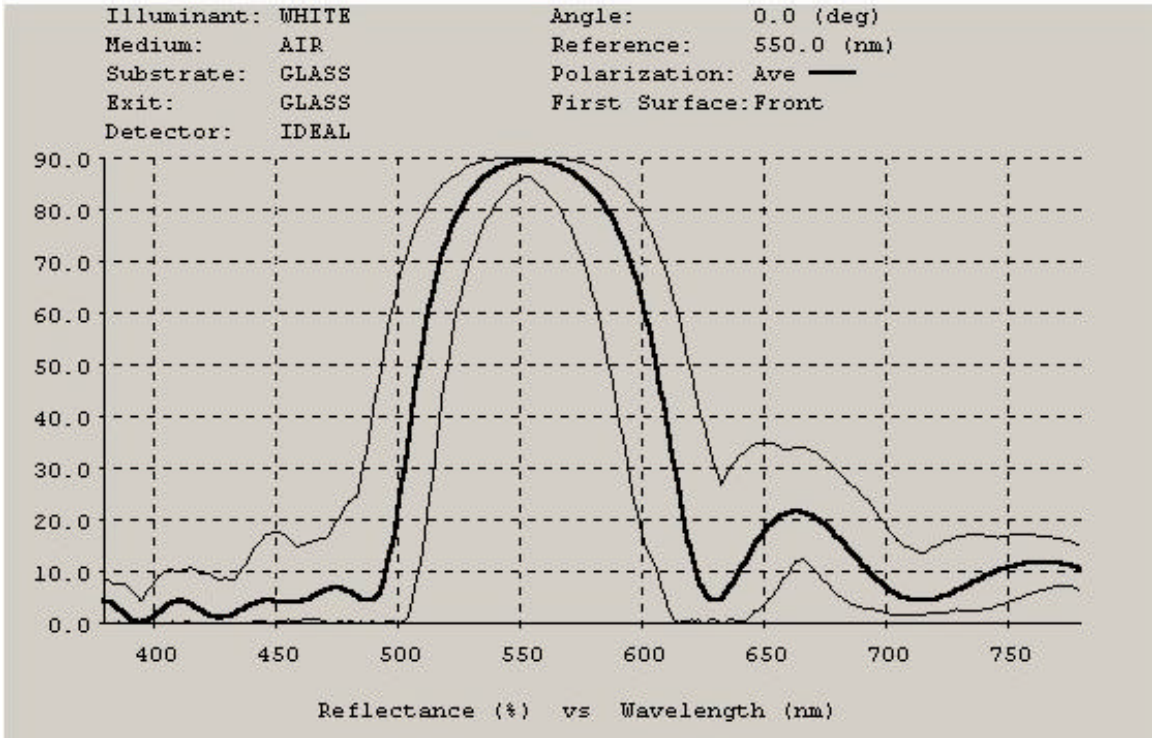

Figure 5-2. Worst case sensitivity curves for a max error of ±5% in thickness.

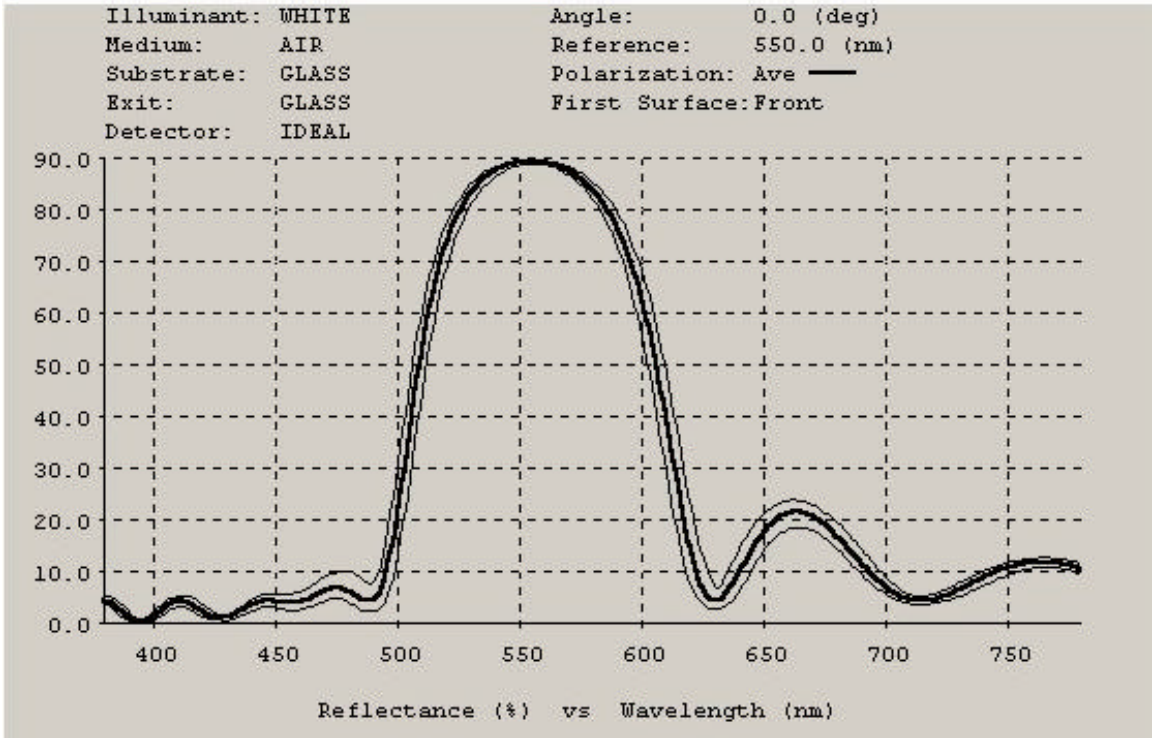

Figure 5-3. Worst case sensitivity curves for a max error of ±1% in thickness.

Figure 5-3 shows the simulated reflectance spectra for this design with a ±1% max error distribution in the thickness of the films and Figure 5-4 shows the same for ±0.2% max error distribution. The refractive index is assumed to be error free for these cases also.

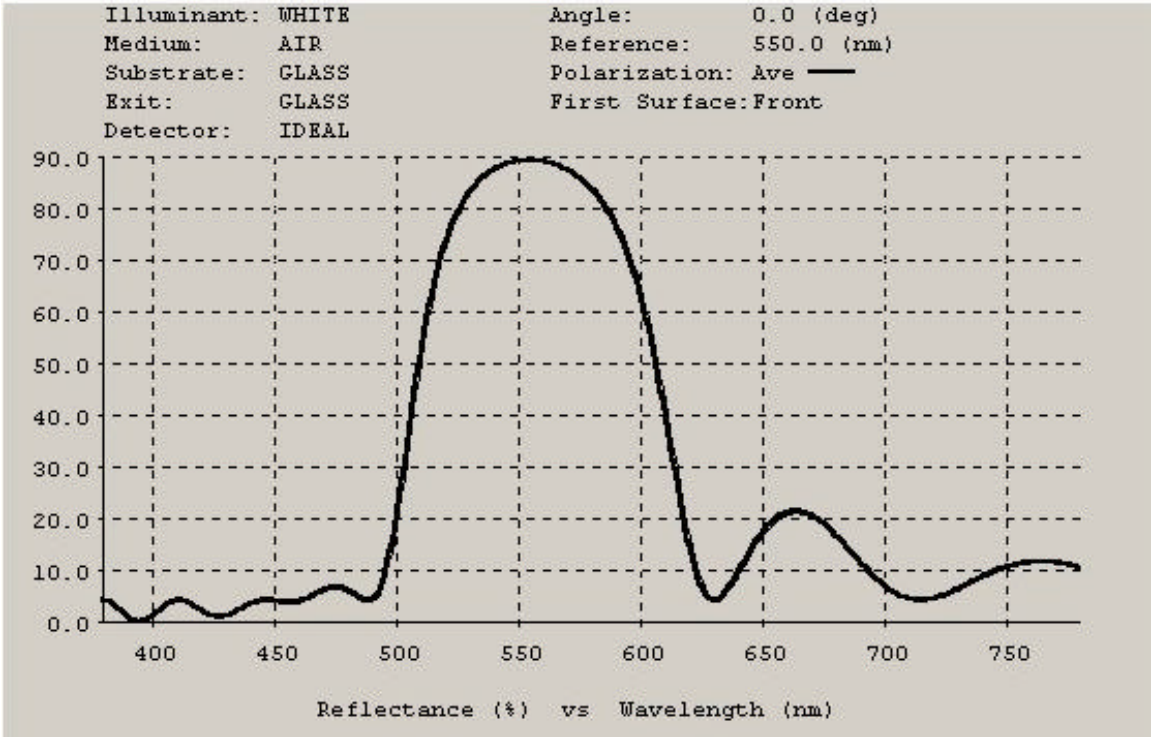

Figure 5-4. Worst case sensitivity curves for a max error of ±0.2% in thickness.

Figure 5-5 shows the simulated reflectance spectra for an error distribution with a maximum of ±5% in the thickness of the layers combined with an error distribution with a maximum of ±1% in the refractive index of the layers. This error of ±1% in the refractive index is an exaggerated value and this does not occur typically. This simulation has been run only to have a general idea of how the changes in refractive index affects the performance of the design.

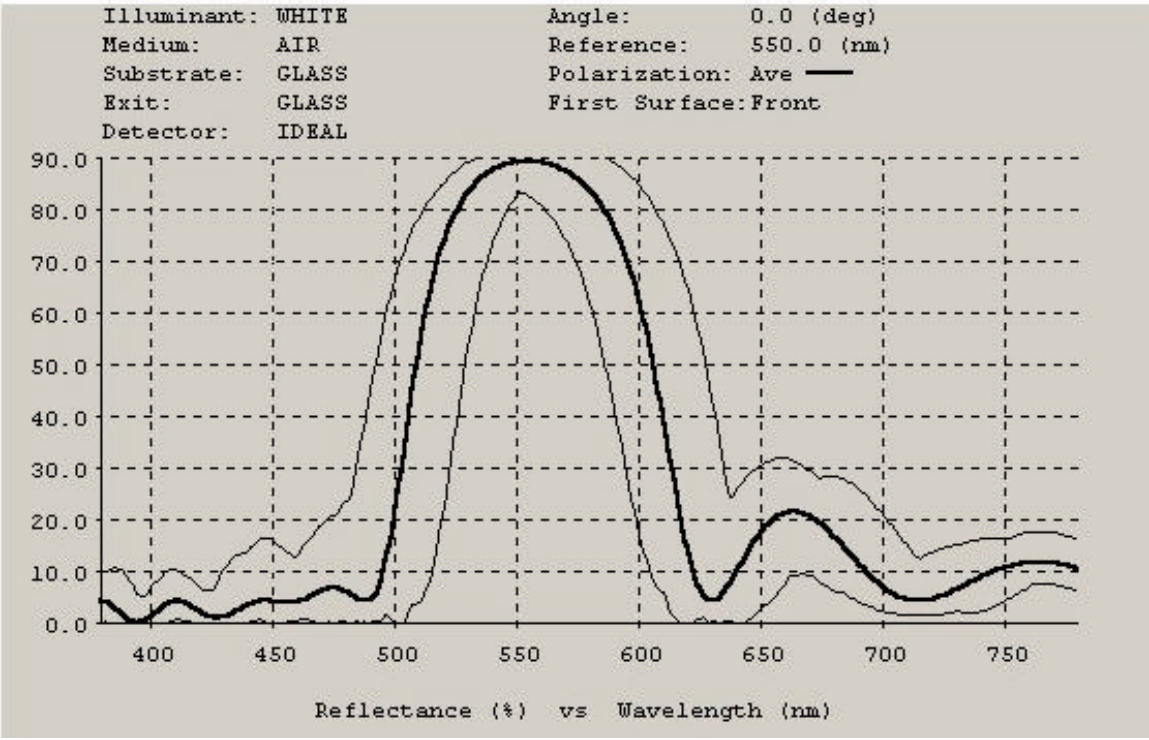

Figure 5-5. Worst case sensitivity curves for a max error of ±5% in thickness and 1% in index.

From Figure 5-5, it can be seen that though the peak wavelength remains almost the same, the pass band for the worst cases undergo an appreciable shift. Thus a 5% error in thickness will lead to considerable deviation in performance from the targeted response. From these simulations, it can be seen that a variation of around 1 to 2% in the thickness of the films will not produce any drastic changes in the reflectance spectrum of the filter. The worst case shows a change in peak wavelength by around ±2nm and the reflectance spectrum does maintain almost the same shape even for the worst case analysis. The changes in wavelength for a maximum error of 1% is even lower and the worst case scenarios are very close to the actual error free spectrum. For a maximum error of 0.2% in thickness of the films, the curves are so close together that it is almost difficult to distinguish between them. So if the error in the ESA process can be brought down to such a value with precise control over the process, then highly reliable filters can be realized. It can also be seen that the error in refractive index of the layers does not affect the shape of the curve, but only changes the absolute values of reflectance.

5.1.2 Design #2

The second quarter wave stack design had the same stack formula of (0.5L H 0.5L)^9, with L being the same material of refractive index 1.4 and H being a material of index 1.85. The center wavelength was taken to be 550nm. The basic symmetric period is repeated 9 times. A white illuminant was used and air with n=1.0 was the incident medium and glass with n=1.52 was the substrate and exit medium. The detector is assumed to be ideal and wideband. The design is centered at a wavelength of 550nm. Figure 5-6 shows the simulated reflectance spectra for this design.

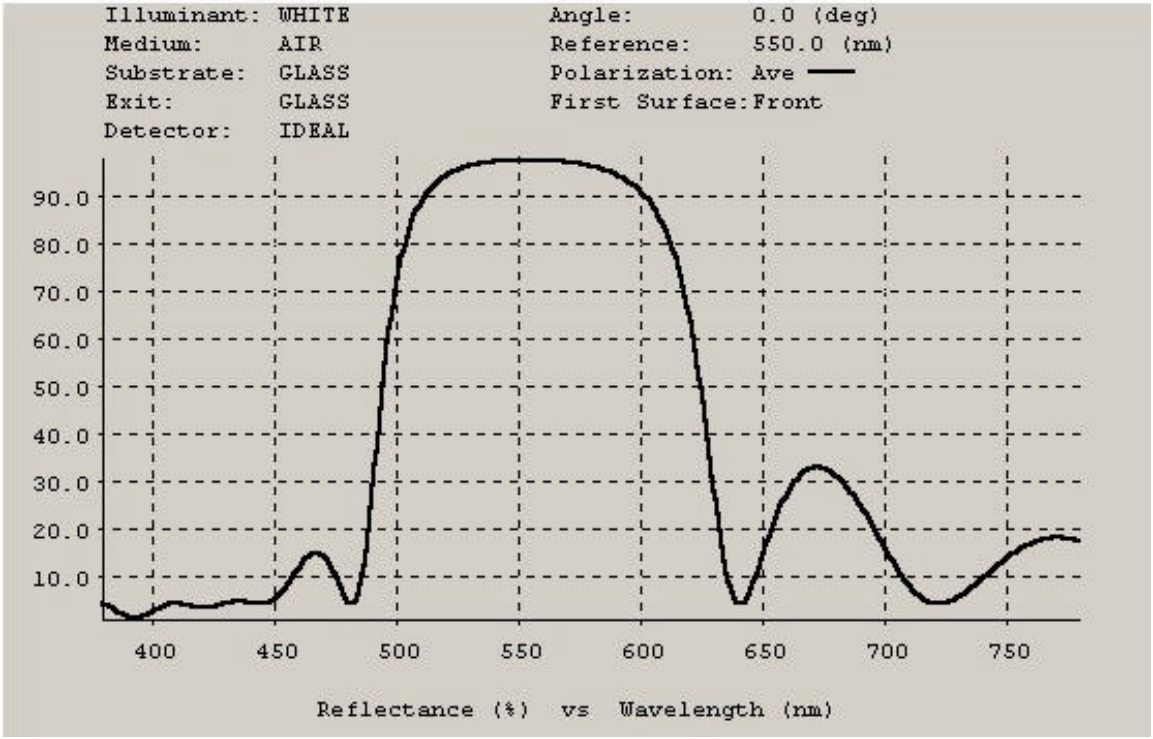

Figure 5-6. Simulated reflectance spectra for design #2.

Figure 5-7 shows the simulated reflectance spectra for this design with a ±5% max error distribution in the thickness of the films, Figure 5-8 the same for ±1% max error in thickness and Figure 5-9 for a 0.2% max error. The refractive index is assumed to be error free for all these cases. Figure 5-10 shows the simulated reflectance spectra for an error distribution with a maximum of ±5% in the thickness of the layers combined with an error distribution with a maximum of ±1% in the refractive index of the layers.

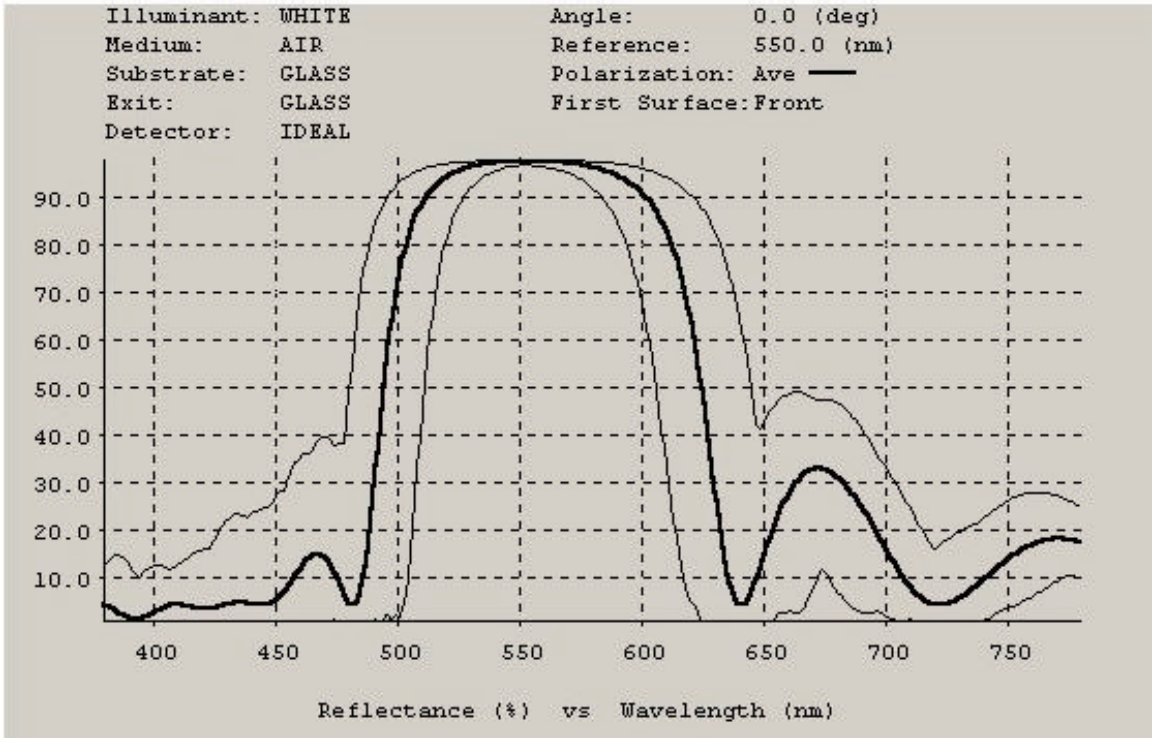

Figure 5-7. Worst case sensitivity curves for a max error of ±5% in thickness.

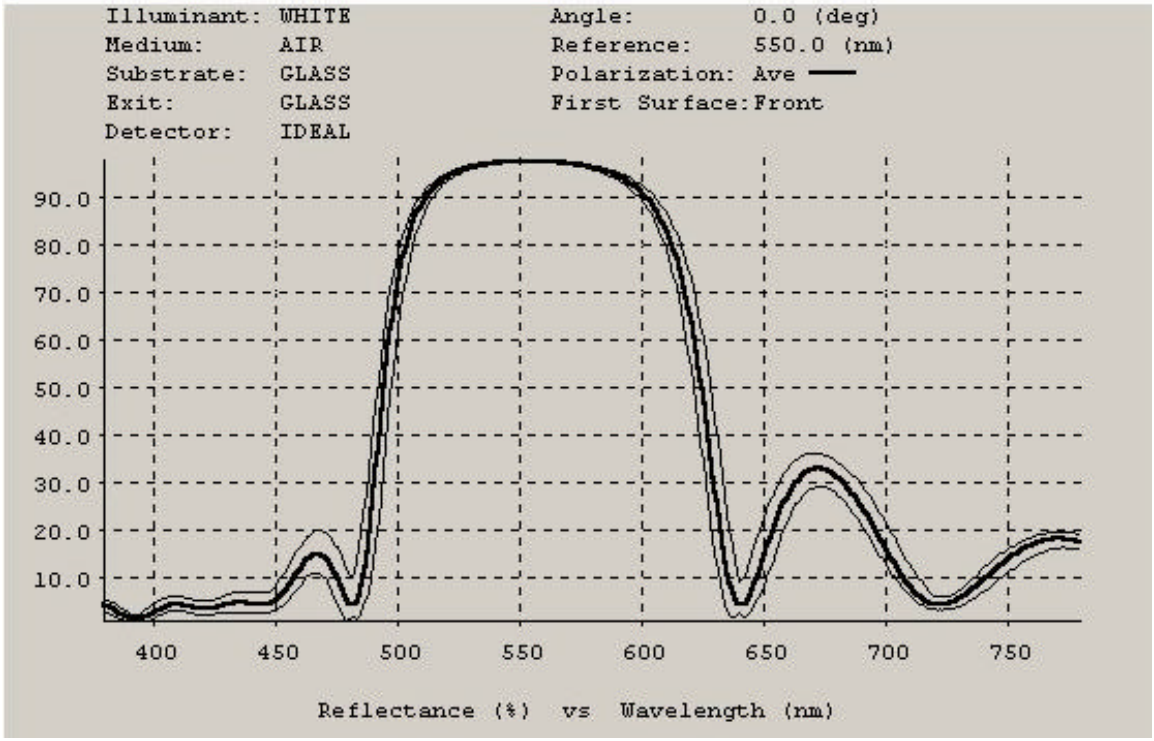

Figure 5-8. Worst case sensitivity curves for a max error of ±1% in thickness.

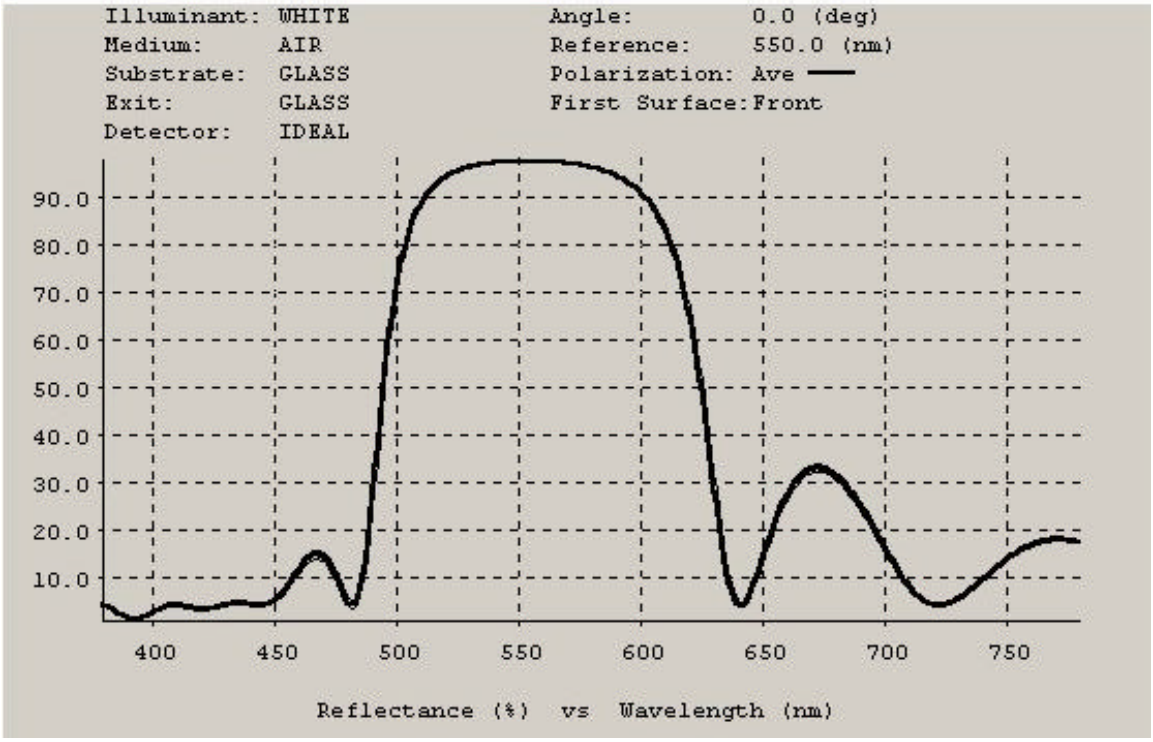

Figure 5-9. Worst case sensitivity curves for a max error of ±0.2% in thickness.

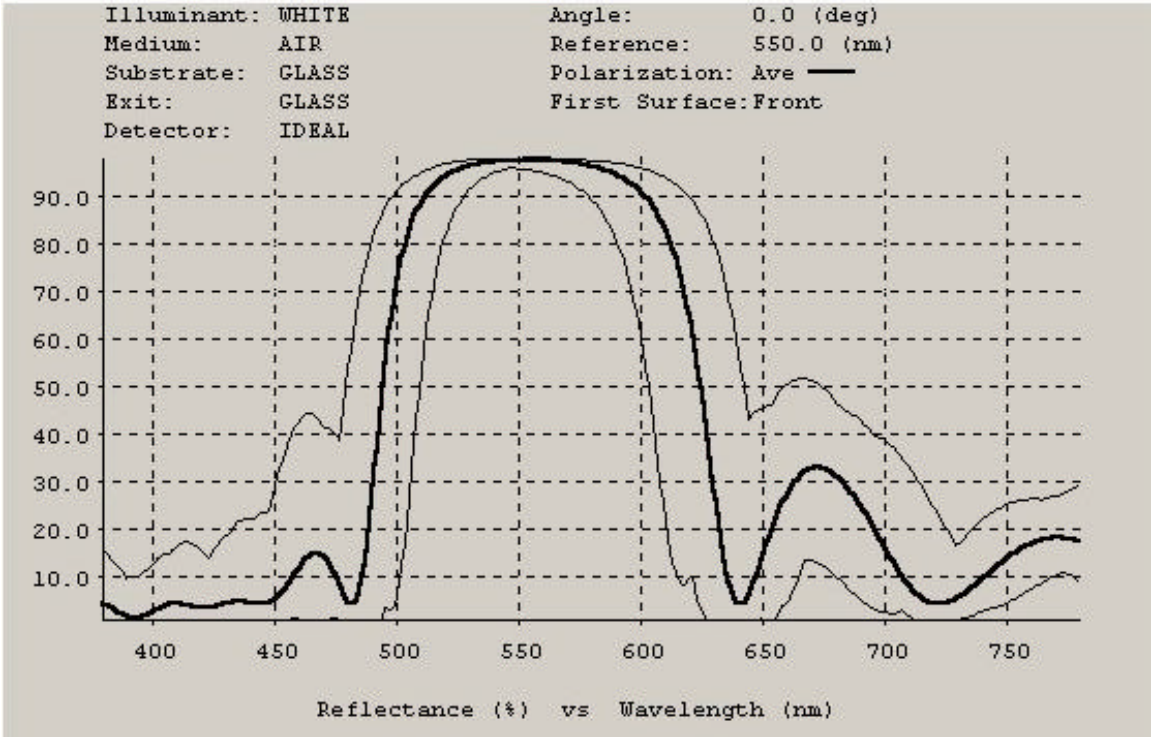

Figure 5-10. Worst case sensitivity curves for a max error of ±5% in thickness and 1% in index.

5.1.3 Design #3

The third quarter wave stack design analyzed had the same stack formula of (0.5L H 0.5L)^9, with L being the same material of refractive index 1.4 and H being a material of index 2.0. The center wavelength was taken to be 550nm. The basic symmetric period is repeated 9 times. A white illuminant was used and air with n=1.0 was the incident medium and glass with n=1.52 was the substrate and exit medium. The detector is assumed to be ideal and wideband. The design is centered at a wavelength of 550nm. Figure 5-11 shows the simulated reflectance spectra for this design.

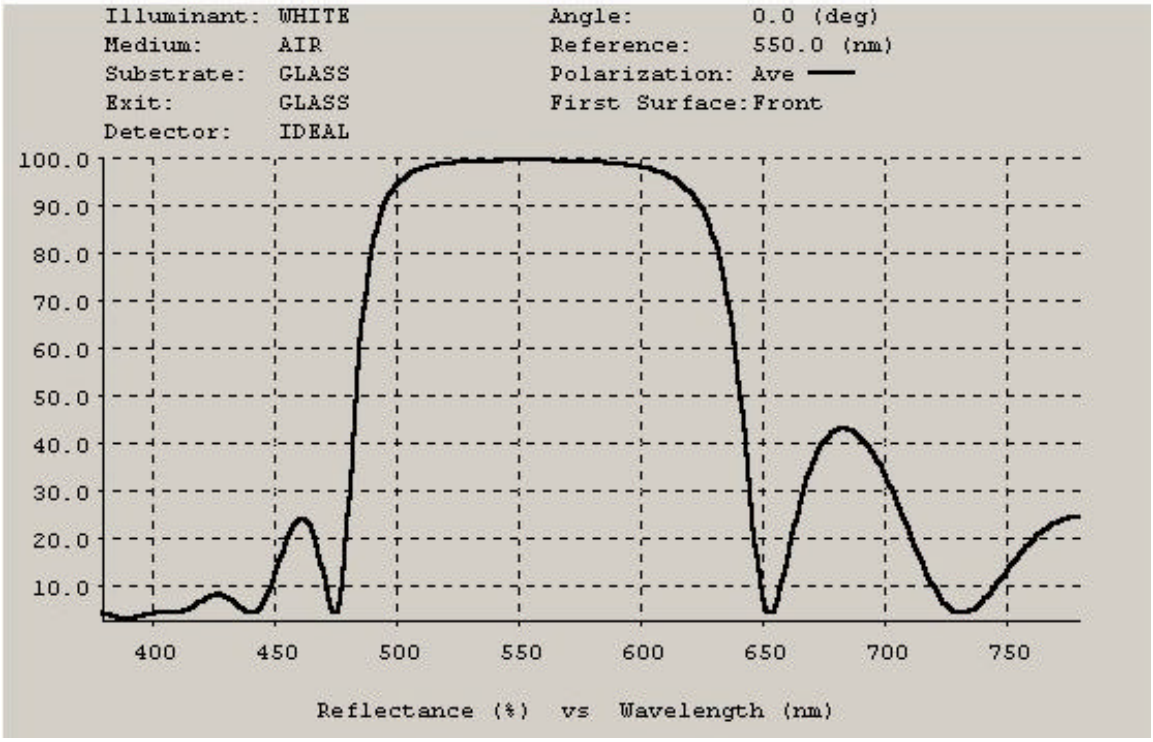

Figure 5-11. Simulated reflectance spectra for design #3.

Figure 5-12 shows the simulated reflectance spectra for this design with a ±5% max error distribution in the thickness of the films, Figure 5-13 the same for ±1% max error in thickness and Figure 5-14 for a 0.2% max error. The refractive index is assumed to be error free for all these cases. Figure 5-15 shows the simulated reflectance spectra for an error distribution with a maximum of ±5% in the thickness of the layers combined with an error distribution with a maximum of ±1% in the refractive index of the layers.

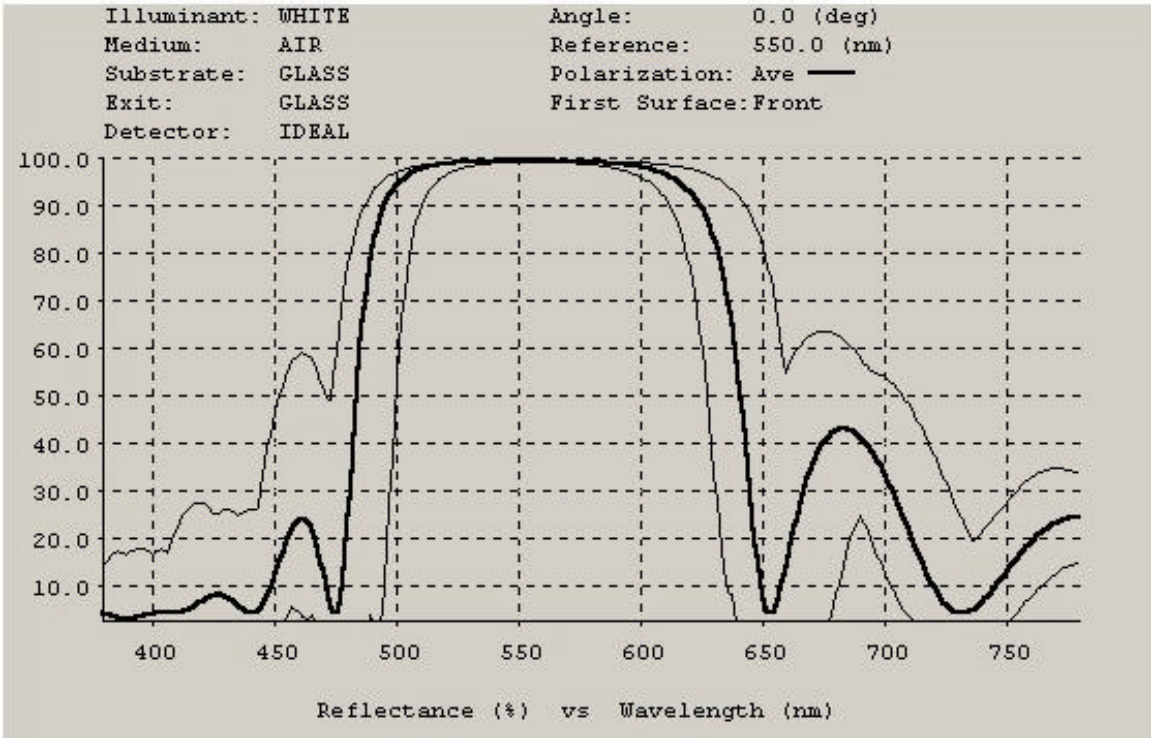

Figure 5-12. Worst case sensitivity curves for a max error of ±5% in thickness.

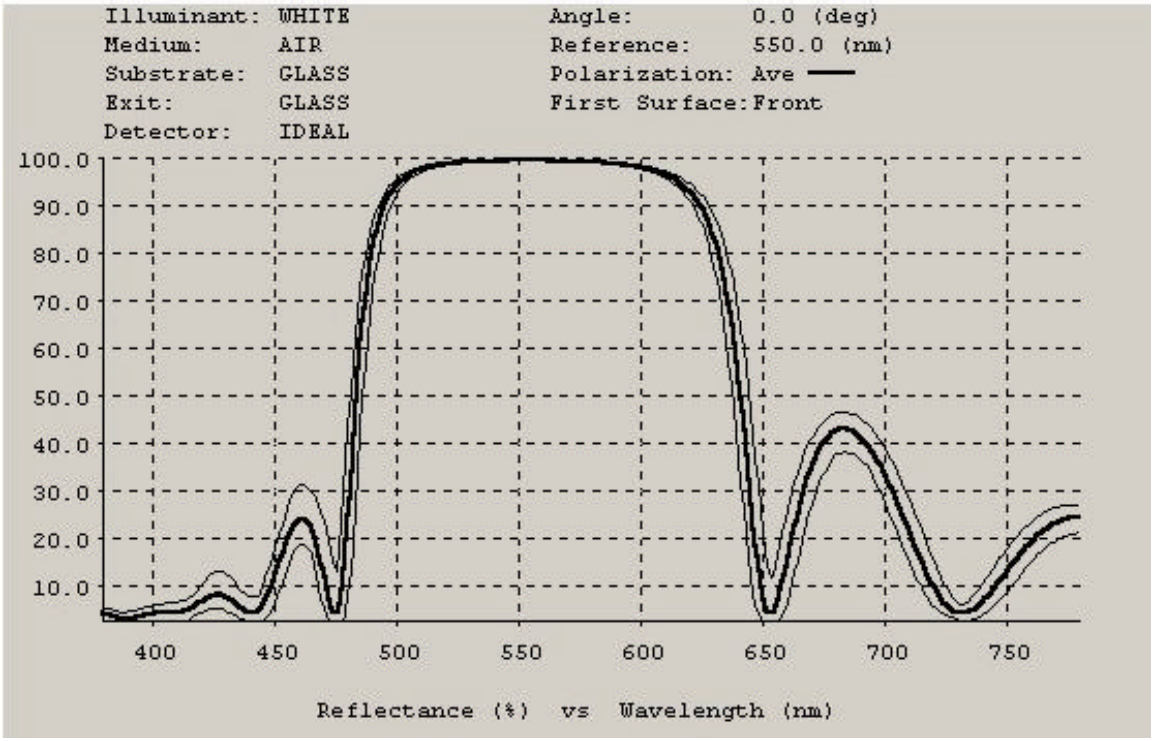

Figure 5-13. Worst case sensitivity curves for a max error of ±1% in thickness.

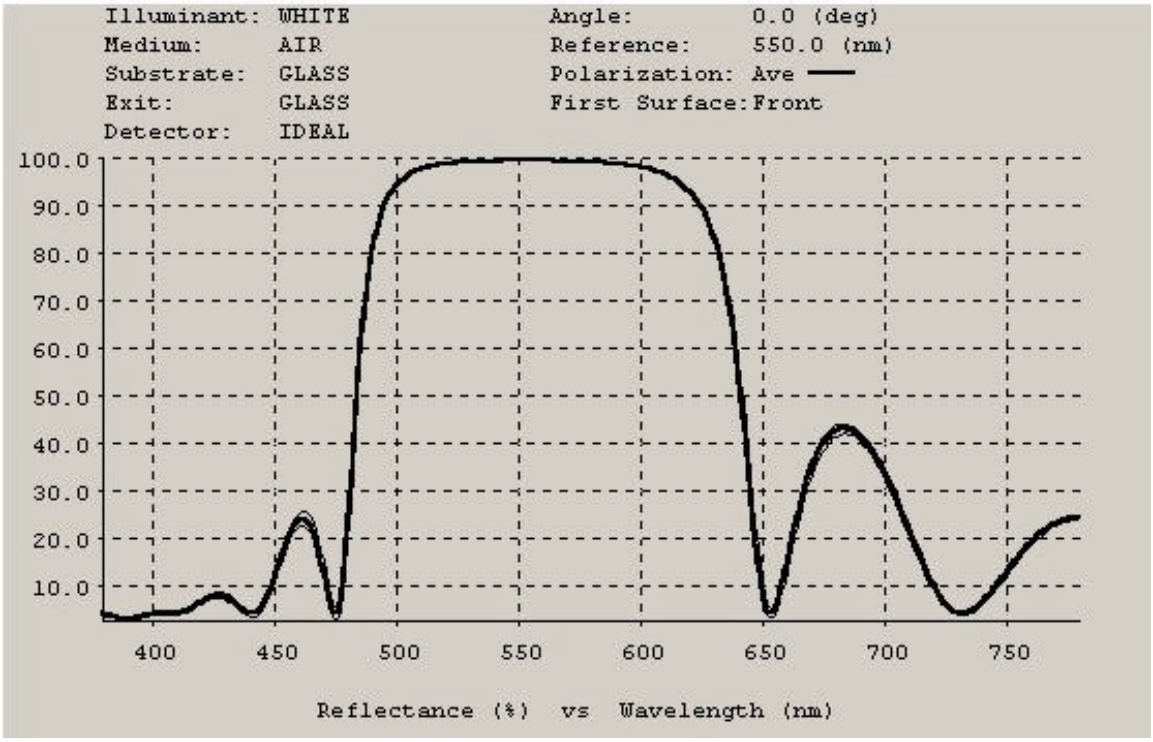

Figure 5-14. Worst case sensitivity curves for a max error of ±0.2% in thickness.

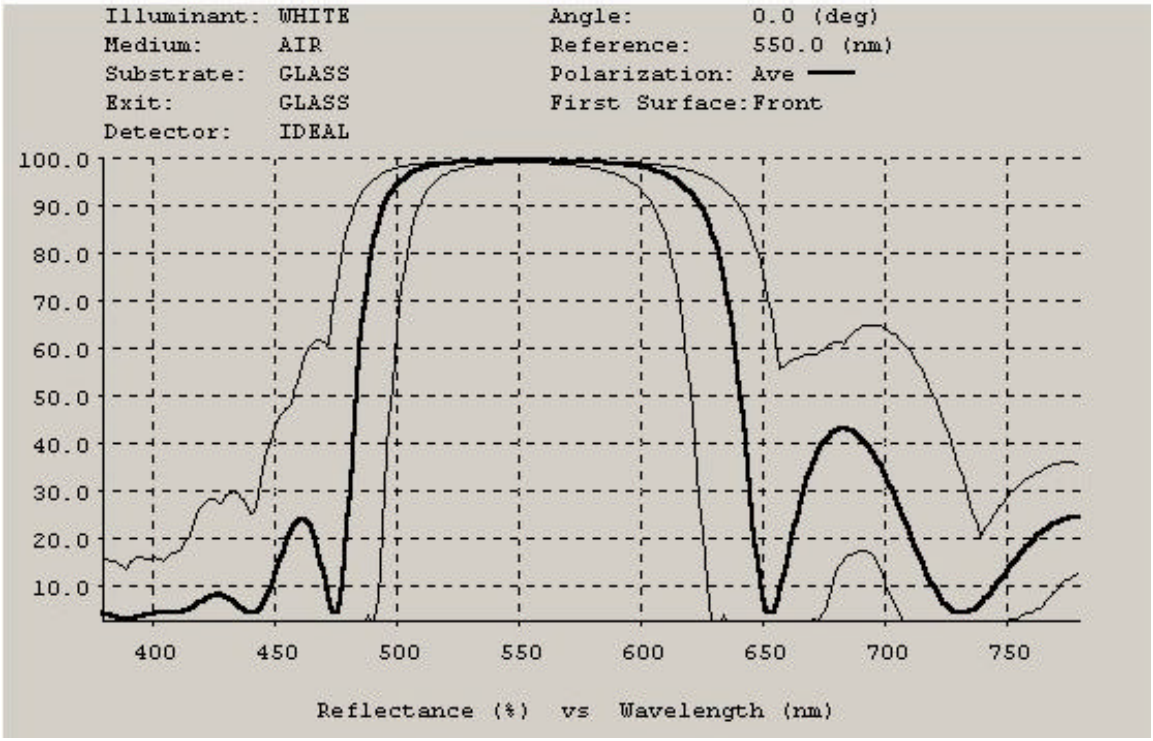

Figure 5-15. Worst case sensitivity curves for a max error of ±5% in thickness and 1% in index.

5.1.4 Design #4

The fourth design analyzed had a quarter wave stack design, with stack formula (0.5L H 0.5L)^15, with L being a material of index 1.4 and H a material of index 2.0. The center wavelength was taken to be 550nm. In design #4, however, the layers were optimized for thickness of the layers and the reflectance between 480nm and 650nm was made one of the targets for optimization and the transmittance between 400 to 450 and from 660 to 750 were made the other targets. The reflectance was targeted to be close to 100% between 480 and 650nm and the transmittance was targeted to be near 100% in the other ranges. The variable matrix method was used for optimization. Figure 5-16 shows the simulated reflectance spectrum for this design.

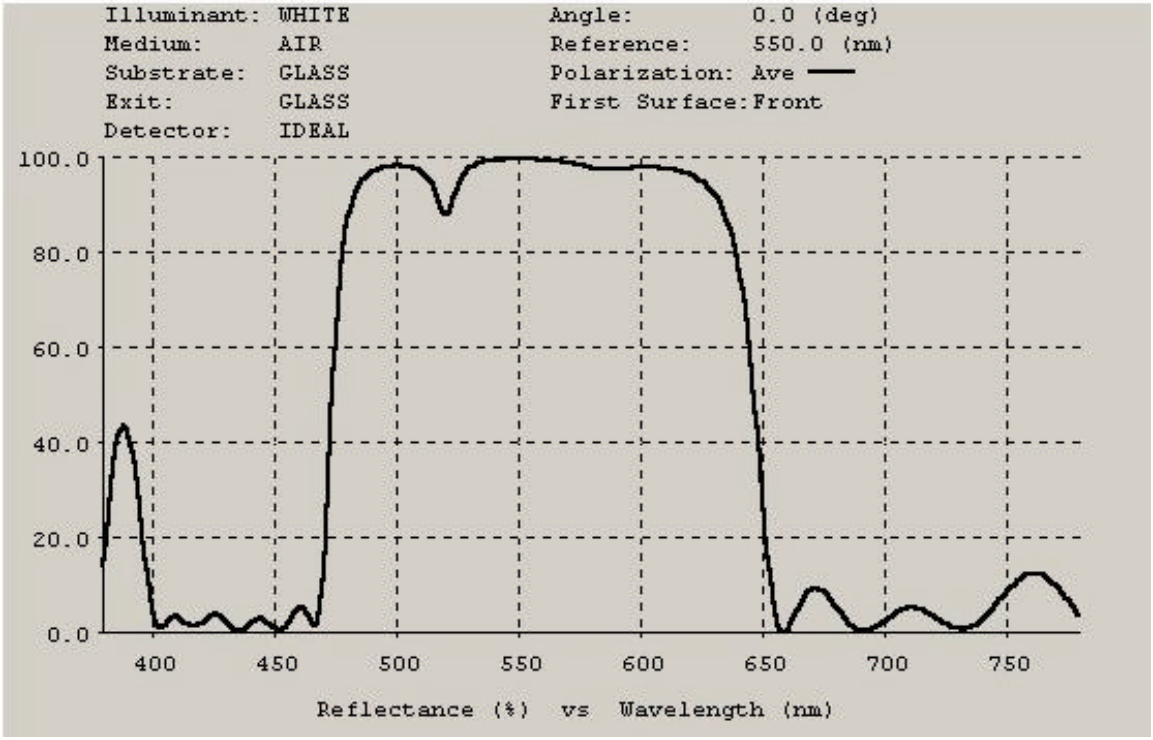

Figure 5-16. Simulated reflectance spectrum for design #4.

Table 5-1 shows the layer thickness for this design after optimization has been done.

Layer	Material	Index	Index Optimize	Thickness (nm)	Thickness Optimize
Layer 1	L	1.4	No	287.2	Yes
Layer 2	H	2.0	No	67	Yes
Layer 3	L	1.4	No	135.49	Yes
Layer 4	H	2.0	No	31.69	Yes
Layer 5	L	1.4	No	36.98	Yes
Layer 6	H	2.0	No	114.33	Yes
Layer 7	L	1.4	No	94.38	Yes
Layer 8	H	2.0	No	45.48	Yes
Layer 9	L	1.4	No	31.5	Yes
Layer 10	H	2.0	No	106.91	Yes
Layer 11	L	1.4	No	96.71	Yes
Layer 12	H	2.0	No	65.48	Yes
Layer 13	L	1.4	No	94.45	Yes
Layer 14	H	2.0	No	66.83	Yes
Layer 15	L	1.4	No	96.42	Yes
Layer 16	H	2.0	No	68.2	Yes
Layer 17	L	1.4	No	98.71	Yes
Layer 18	H	2.0	No	70.26	Yes
Layer 19	L	1.4	No	102.17	Yes
Layer 20	H	2.0	No	72.11	Yes
Layer 21	L	1.4	No	186.25	Yes
Layer 22	H	2.0	No	15.07	Yes
Layer 23	L	1.4	No	91.35	Yes
Layer 24	H	2.0	No	106.75	Yes
Layer 25	L	1.4	No	86.75	Yes
Layer 26	H	2.0	No	73.76	Yes
Layer 27	L	1.4	No	134.96	Yes
Layer 28	H	2.0	No	35.39	Yes
Layer 29	L	1.4	No	56.16	Yes
Layer 30	H	2.0	No	112.57	Yes
Layer 31	L	1.4	No	0	Yes

Table 5-1. Layer thickness and index of design #4 after optimization has been done.

Figure 5-17 shows the simulated reflectance spectra for this design with a ±5% max error distribution in the thickness of the films, Figure 5-18 the same for ±1% max error in thickness and Figure 5-19 for a 0.2% max error. The refractive index is assumed to be error free for all these cases. Figure 5-20 shows the simulated reflectance spectra for an error distribution with a maximum of ±5% in the thickness of the layers combined with an error distribution with a maximum of ±1% in the refractive index of the layers.

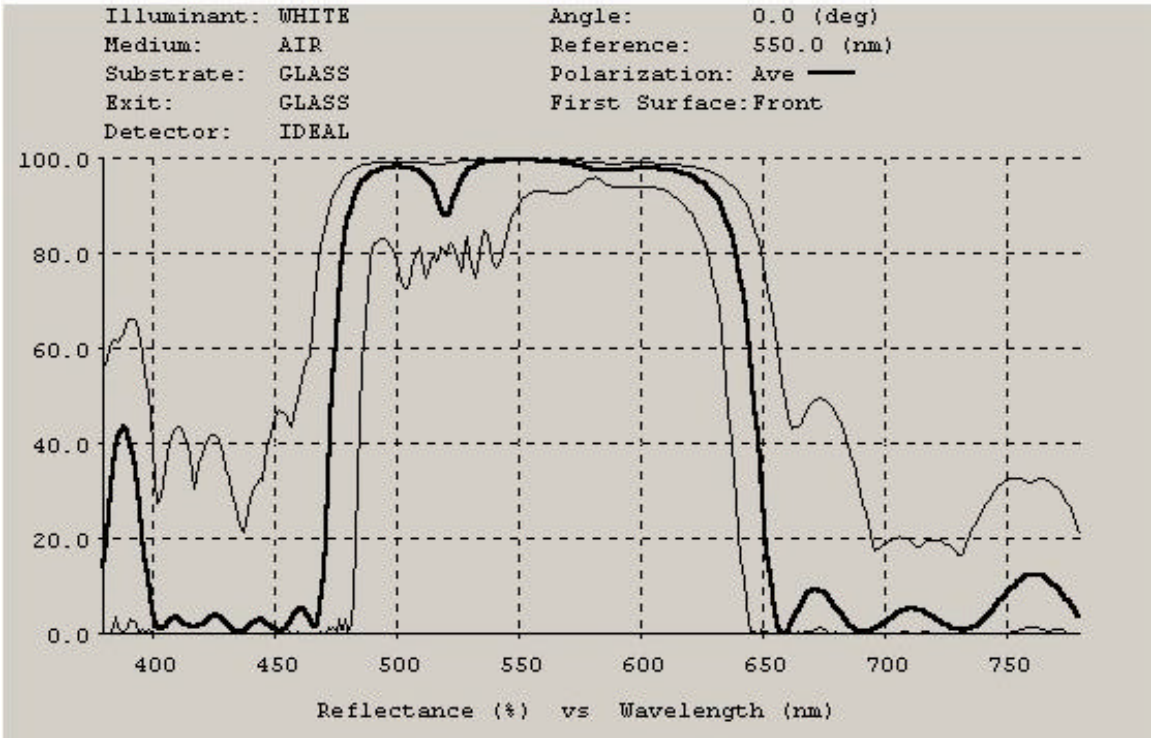

Figure 5-17. Worst case sensitivity curves for a max error of ±5% in thickness.

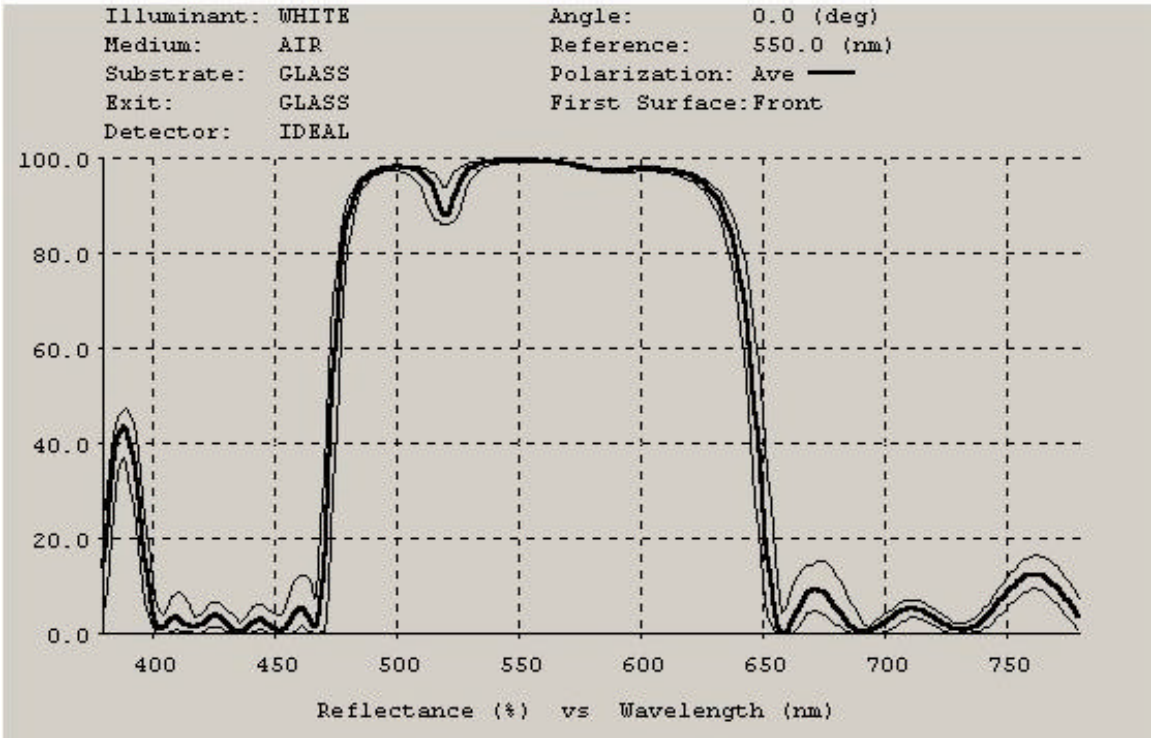

Figure 5-18. Worst case sensitivity curves for a max error of ±1% in thickness.

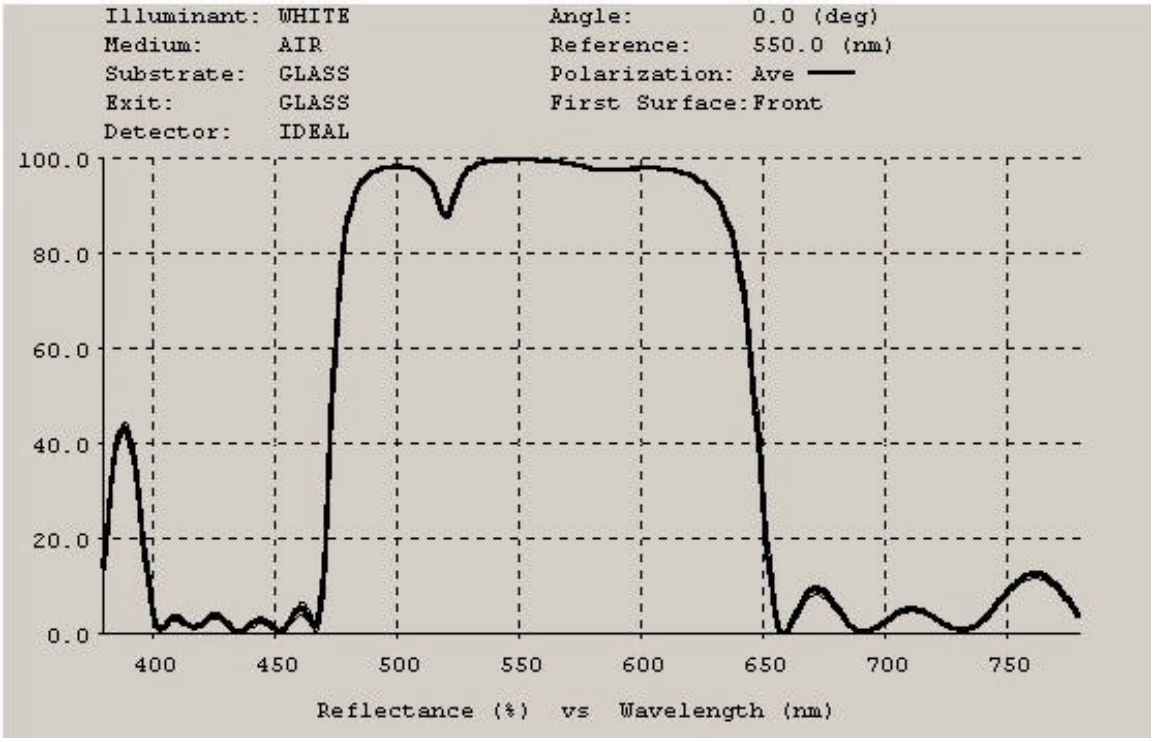

Figure 5-19. Worst case sensitivity curves for a max error of ±0.2% in thickness.

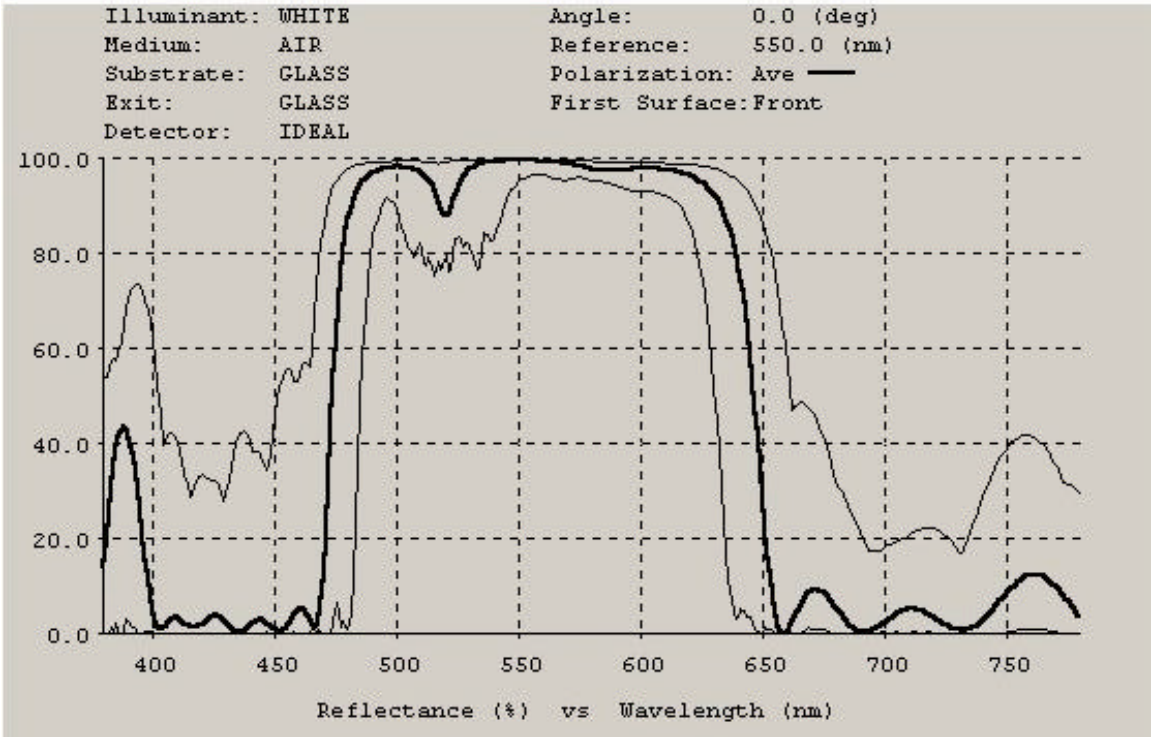

Figure 5-20. Worst case sensitivity curves for a max error of ±5% in thickness and 1% in index.

5.2 Conclusions

From the sensitivity analysis done it can be safely assumed that the ESA process with a maximum of only about ± 1 to ±2% thickness error provides a highly reliable method of fabricating thin films for filter design. As the ratio of refractive indices increases it can be seen that the same percentage error in thickness causes a slightly higher error in wavelength response. When the error in thickness goes up to about ±5% the shift in the pass band of the filter varies as much as 100%. If with proper control and quality checks, the total error of the ESA process can be maintained at a value around 1% to 2%, which is a highly practical and attainable value, the error introduced due to the process (errors in thickness) will be negligible. Errors in index are not caused by the ESA process per se and so do not contribute appreciably in the sensitivity filter response.

Chapter 6 A Hot Mirror Design

6.1 Requirements

The objective of this exercise is to design an edge filter to block the higher wavelength region of the spectrum while passing shorter wavelengths. The filter should have near 0% reflectance from around 250 to 400nm and near 100% reflectance from 400 to around 2000nm. This filter is to be coated on the lenses of spectroscopes used to analyze radiation emanating from rocket engines, to understand the combustion process. The filter blocks out the part of the spectrum containing the heat and protects the instrument from overheating and burning out. The radiation from 250 to around 400nm is the radiation of interest which needs to be analyzed by the spectrometer, so it should be completely passed. The problem encountered is that since the operating temperature is very high, around 500^0 C, most existing filters cannot survive this extreme heat.

6.2 Approach Used

Since the filter is to be designed to work at extremely high temperatures, the materials used for these filters should not only be capable of withstanding these temperatures, but also be able to maintain the optical characteristics required. Also, since the bandwidth of the rejection band is very high, the ratio of refractive indices between the materials needs to be as high as possible. When high temperature sintering takes place, it affects the thickness of the films as well as the refractive index of the films. So materials that were chosen for making these films were sintered at a temperature of 1000^0 C, which is much higher than its anticipated operating temperature, in an oven to find the effects of high temperature on these thin films. The materials chosen were ZrO_2, as the high index material and Al_2O_3 as the low index material. Table 6-1 shows the data for these materials before and after sintering. These materials were chosen because of the materials analyzed, these were the materials which gave the most consistent results after sintering and these were the materials which produced the most uniform films.

Material	Average thickness per bilayer before sintering (nm)	Average refractive index per bilayer before sintering	Average thickness per bilayer after sintering (nm)	Average refractive index per bilayer after sintering
ZrO_2 concentration 10mg/ml	0.977	1.578	0.309	1.759
Al_2O_3 concentration 20mg/ml	2.42	1.493	2.144	1.389

Table 6-1. Material data before and after sintering.

From the table it is obvious that the thickness of ZrO_2 reduce to around one third the original value after sintering and the refractive index rises slightly. For the Al_2O_3 film the change in thickness is not appreciable and the index is reduced slightly after sintering. So it is obvious that sintering will compress the filter dimensions.

The approach towards designing and producing these filters was as follows. A design for the required characteristics is performed using the post sintered values of refractive indices (H = 1.59 and L = 1.389) and TFCalc software. In order to obtain the correct layer thickness after sintering, the ZrO_2 layers are fabricated nearly three times as thick as the designed values and the Al_2O_3 layers are fabricated about 1.13 times thicker than the designed value. Then the whole assembly is sintered, so that the layer thickness becomes equal to the designed values. That is, we make a thicker filter than necessary, and by proper modeling we make sure that we have the final correct dimensions after sintering. Since the filter is sintered at a temperature much higher than the anticipated operating temperature, it should be able to survive the lower operating temperature without any problems.

6.3 Design and Optimization

Using the approach as defined in the previous section, the filter was designed using TFCalc, taking the higher index material, represented by H, having a refractive index of 1.759 and the lower index material represented by L, with a refractive index of 1.389. The following stack formula was used to generate the stack.

(0.457L 0.913H 0.457L)^6 (0.5L H 0.5L)^6 (0.52L 1.04H 0.52L)^3

(0.61L 1.22H 0.61L)^9 (0.674L 1.347H 0.674L)^3 (0.75L 1.5H 0.75L)^9

(0.6L 2.4H 0.6L)^9 (0.659L 2.637H 0.659L)^9

(0.647L 1.481H 0.177L 1.481H 0.647L)^11

(0.695L 1.589H 0.190L 1.589H 0.695L)^11 ,

with 475 nm as the center wavelength. L and H in the stack formula represent a quarter wave film of the material. Glass was used as the substrate and exit medium, and air was the incident medium. An ideal detector function was assumed. Figure 6-1 shows the filter response obtained for the above stack formula, without optimization.

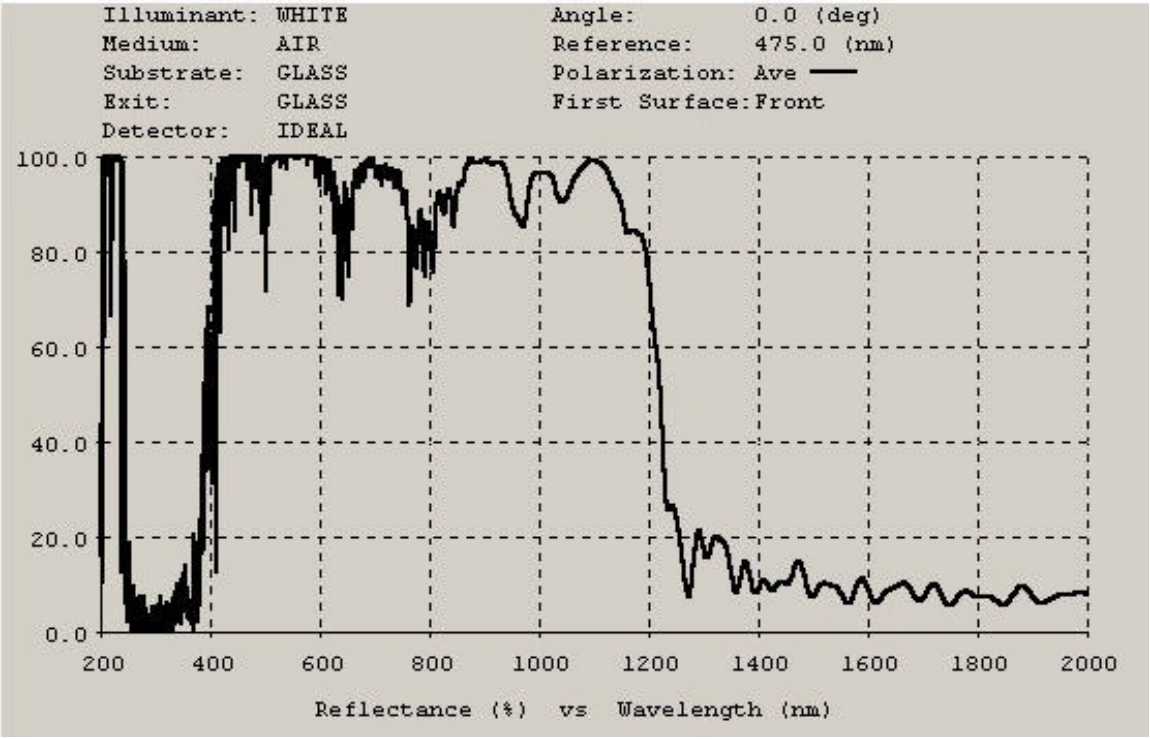

Figure 6-1. Filter response of the heat reflector filter design without optimization.

This design was then optimized using the variable metric method. The reflectance between 400 and 2000nm was targeted to be 100% and the reflectance between 230 and 400nm was targeted to be 0%. Optimization was done using the variable metric method. Figure 6-2 shows the targets specified for optimization. All the layers were optimized for thickness.

Targets - Continuous

Options

Target #	1	2	3	4	5	6	7
Kind	Intensity	Intensity	Intensity	Intensity	Intensity	Intensity	Intensity
Refl/Tran	Refl	Refl	Refl	Refl	Refl	Refl	Refl
Polarization	Ave	Ave	Ave	Ave	Ave	Ave	Ave
Wavelength (begin)	250.0	400.0	450.0	260.0	300.0	310.0	350.0
Wavelength (end)	390.0	1700.0	800.0	300.0	390.0	350.0	375.0
Angle	0.0	0.0	0.0	0.0	0.0	0.0	0.0
Target (begin)	5.0	100.0	100.0	2.0	2.0	1.0	0.0
Target (end)	5.0	100.0	100.0	2.0	2.0	1.0	0.0
Tolerance	0.001	0.01	0.001	0.001	0.001	0.001	0.001
Environment	1	1	1	1	1	1	1

Figure 6-2. Optimization Targets.

Figure 6-3 shows the spectral filter characteristics after optimization is performed.

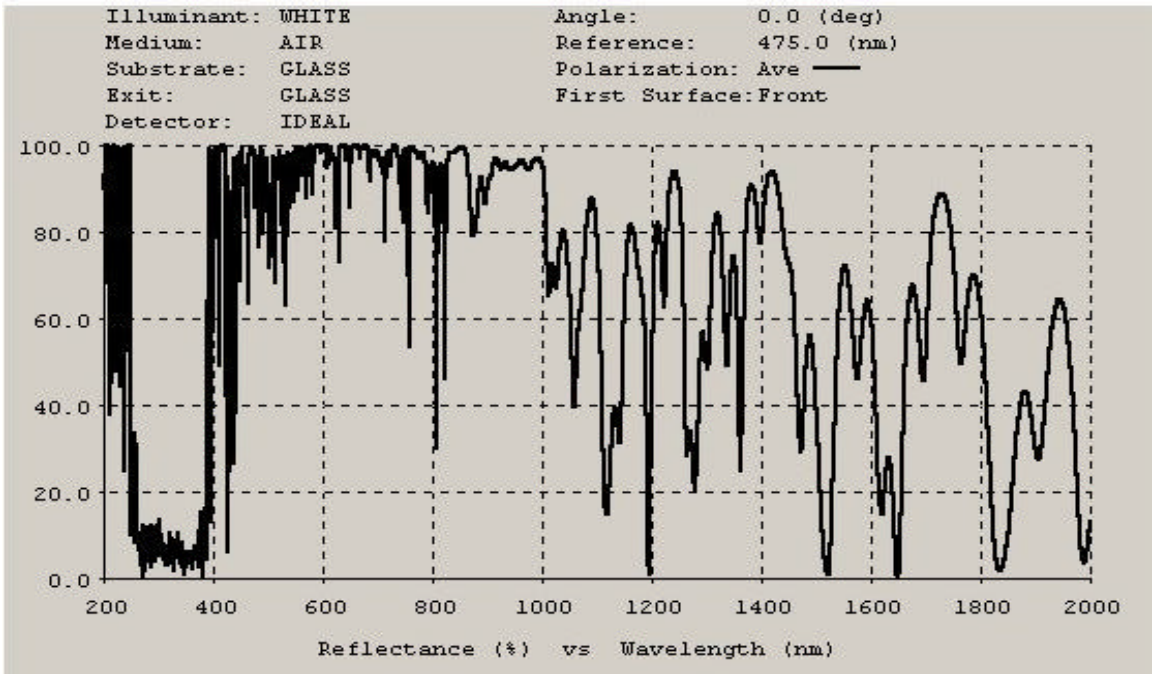

Figure 6-3. Spectral Response after optimization.

Layer data for this design after optimization is given in Table 6-2. In Table 6-2, L represents the low index material which is Al_2O_3 and H represents High index material which is ZrO_2.

Material	Layer Thickness
L	0
H	97.46
L	19.6
H	89.01
L	86.22
H	68.92
L	89.95
H	75.09
L	0
H	89.96
L	123.61
H	12.71
L	152.42
H	0
L	70.33
H	76.77
L	90.48
H	77.91
L	104.41
H	77.56
L	93.76
H	68.92
L	97.06
H	50.84
L	0
H	122.98
L	119.43
H	101.5
L	126.44
H	99.57
L	109.75
H	72.59
L	93.72
H	68.17
L	94.07
H	73.96
L	111.43
H	98.47
L	122.7
H	93.64
L	104.96
H	73.8
L	91.09
H	71.86
L	94.46

H	86.34
L	123.58
H	99.59
L	129.02
H	99.68
L	127.83
H	90.34
L	95.96
H	82.5
L	225.05
H	83.65
L	96.5
H	87.59
L	127.61
H	100.67
L	126.4
H	99.78
L	112.11
H	81
L	116.03
H	99.31
L	127.33
H	102.61
L	129.53
H	101.91
L	125.23
H	101.62
L	117.97
H	168.49
L	101.36
H	157.55
L	99.51
H	154.31
L	98.14
H	153.94
L	98.26
H	156.95
L	98.17
H	157.16
L	100.61
H	158.52
L	105.76
H	175.85
L	116.27
H	181.75
L	112.91
H	181.75
L	111.18
H	170.07
L	104.24
H	163.16
L	101.7
H	160.15

L	104.37
H	258.15
L	110.53
H	180.38
L	118.89
H	183.86
L	113.24
H	183.38
L	118.47
H	173.35
L	106.31
H	82.27
L	0
H	78.27
L	105.88
H	140.83
L	0
H	115.14
L	111.47
H	148.32
L	0
H	111.73
L	111.41
H	134.28
L	0
H	127.62
L	115.08
H	110.19
L	6.23
H	154.04
L	0
H	153.29
L	6.46
H	111.56
L	114.9
H	0
L	0
H	208.01
L	0
H	177.25
L	115.76
H	0
L	118.59
H	196.02
L	0
H	50.92
L	119.79
H	144.43
L	0
H	173.12
L	0
H	90.96
L	127.57

H	20.3
L	123.36
H	137.58
L	0
H	125.62
L	108.76
H	132.19
L	0
H	129.58
L	107.1
H	135.34
L	0
H	127.49
L	109.93
H	153.3
L	0
H	110.36
L	318.4
H	133.88
L	0
H	160.07
L	99.95
H	189.02
L	0
H	177.85
L	107.54
H	103.35
L	0
H	157.43
L	107
H	183.92
L	0
H	74.8
L	107.94
H	109.04
L	0
H	151.55
L	105.48
H	144.32
L	0
H	116.8
L	223.23
H	76.68
L	0
H	183.84
L	54.59

Table 6-2. Layers and Thickness after Optimization.

Even after optimization, using a large number of overlapping targets, the spectral response does not exactly replicate the requirements. The transmission between 250 and

400nm is very high and the average reflectance between 400 nm and 200nm is high but not very uniform.

6.4 Summary

A filter for a specific application was designed and optimized using TFCalc software. Due to the high temperature application of the material, the materials used were sintered at a much higher temperature and this data was used to design the filter. Optimization of the design using TFCalc produced better though not perfect results.

Chapter 7 Factors Affecting Filter Response

All the designs and simulations till this point were carried out assuming normal incidence and average polarization of incident light. The angle of incidence and polarization of incident light will change the spectral response of the filter. The effect of these on the response of thin film coatings would be valuable in that it would help to make these films respond in the same way irrespective of the angle of incidence or the polarization of incident light.

7.1 Incident Angle and Polarization

The angle at which light is incident on the thin film plays an important role in determining the spectral response of the film. From the analysis carried out in chapter 3, the reflectance and transmittance for normal incidence for a simple interface between two media were found to be

$r_s = -r_p = \frac{n_i - n_t}{n_i + n_t}$ and $t_s = t_p = \frac{2n_i}{n_i + n_t}$, respectively. For oblique incidence, these become

$r_s = \frac{n_i \cos\theta_i - n_t \cos\theta_t}{n_i \cos\theta_i + n_t \cos\theta_t}$ and $t_s = \frac{2n_i \cos\theta_i}{n_i \cos\theta_i + n_t \cos\theta_t}$ for s polarization and

$r_p = \frac{n_t \cos\theta_i - n_i \cos\theta_t}{n_i \cos\theta_t + n_t \cos\theta_i}$ and $t_p = \frac{2n_i \cos\theta_i}{n_i \cos\theta_t + n_t \cos\theta_i}$ for p polarization,

where θ_i is the incident angle and θ_t is the transmitted angle. The reflectance $R_s = r_s^2$ and the transmittance $T_s = 1-R_s$ for s polarization and $R_p = r_p^2$ and $T_p = 1-R_p$ for p polarization. So, as the incident angle and the polarization change, the values of reflectance and transmittance vary for a simple interface. The same is the case for a thin film structure. In all the analysis done till this point in this thesis, normal incidence and average polarization (50% s and 50% p polarization) has been assumed, which is usually not the case in practical applications. Practical applications usually have light incident on the filter at non-normal angles of incidence and in some special applications incident light could be of either s or p polarization. To understand the effect of polarization and incident angle on the spectral response, a small example is considered.

7.1.1 Example

A multilayer dielectric stack filter design using the stack formula (0.5L H 0.5L)^9 has been considered. The materials used in this simulation are MgF_2 which is represented by L in the stack formula and TiO_2 which is represented by H. MgF_2 has a refractive index of 1.38 and TiO_2 has a refractive index of 2.385 at the central wavelength of 550nm. Air is the incident medium and glass of refractive index 1.52 is the exit medium. An ideal detector function is assumed. Figure 7-1 shows the response of this design to normal incidence of light.

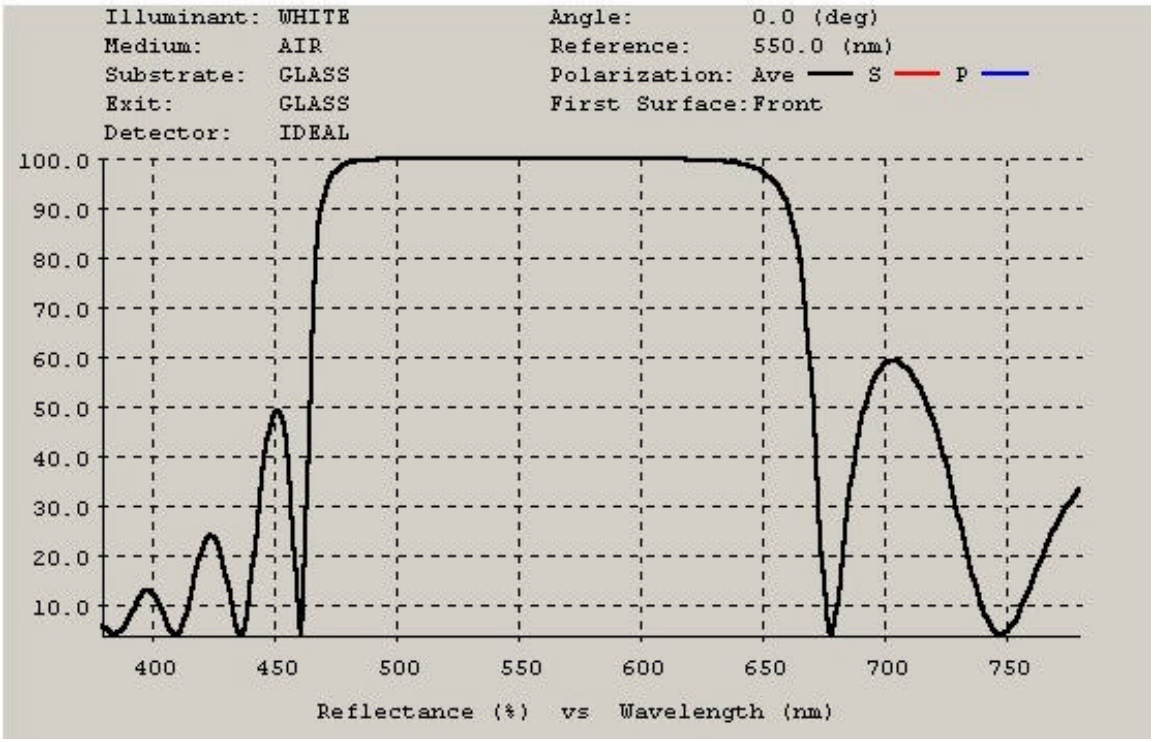

Figure 7-1. Filter response to normal incidence.

As it can be seen from the figure the response for s and p polarization are the same and is equal to average polarization at normal incidence. Figure 7-2 shows the response of the filter when light is incident at 20^0 to the normal. Figure 7-3 shows the response for light incident at 40^0 and Figure 7-4 shows the response for light incident at 60^0 to the normal. Figure 7-5 shows the response for average polarization of light incident at 0^0, 20^0, 40^0, and 60^0 to the normal. The curve at the extreme right in Figure 7-5 is the one showing the response for normal incidence and the one at the extreme left shows the response for 60^0 incidence.

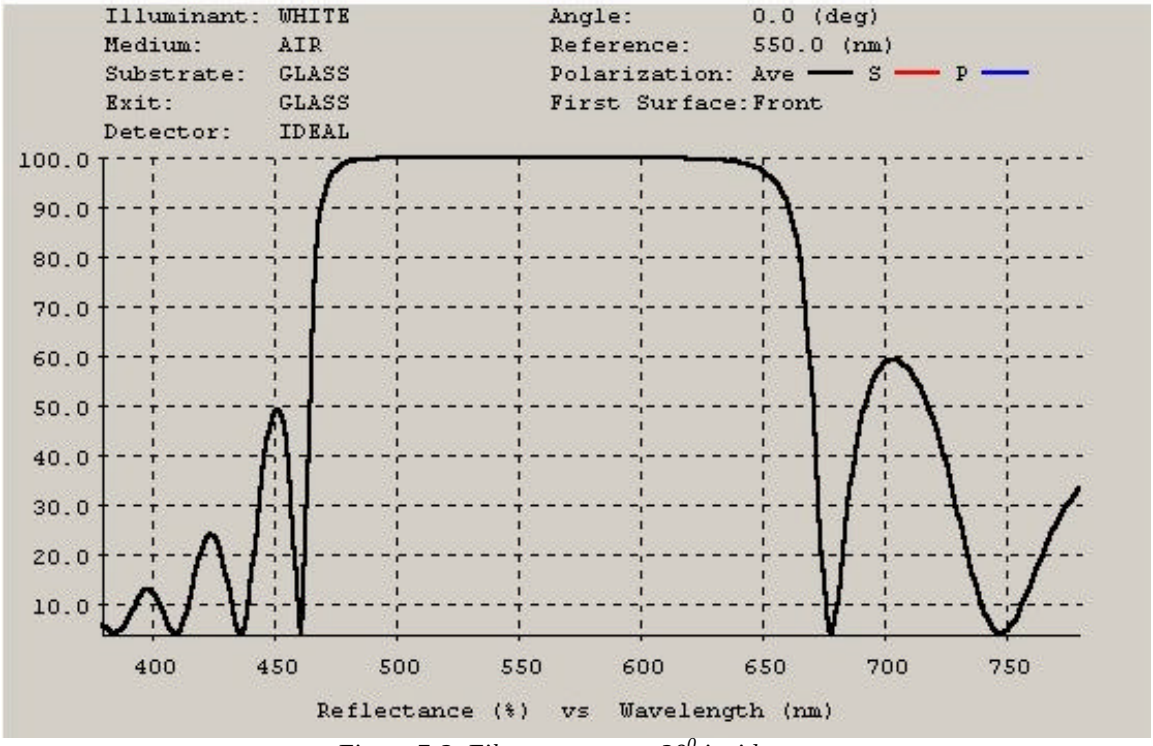

Figure 7-2. Filter response to20^0 incidence.

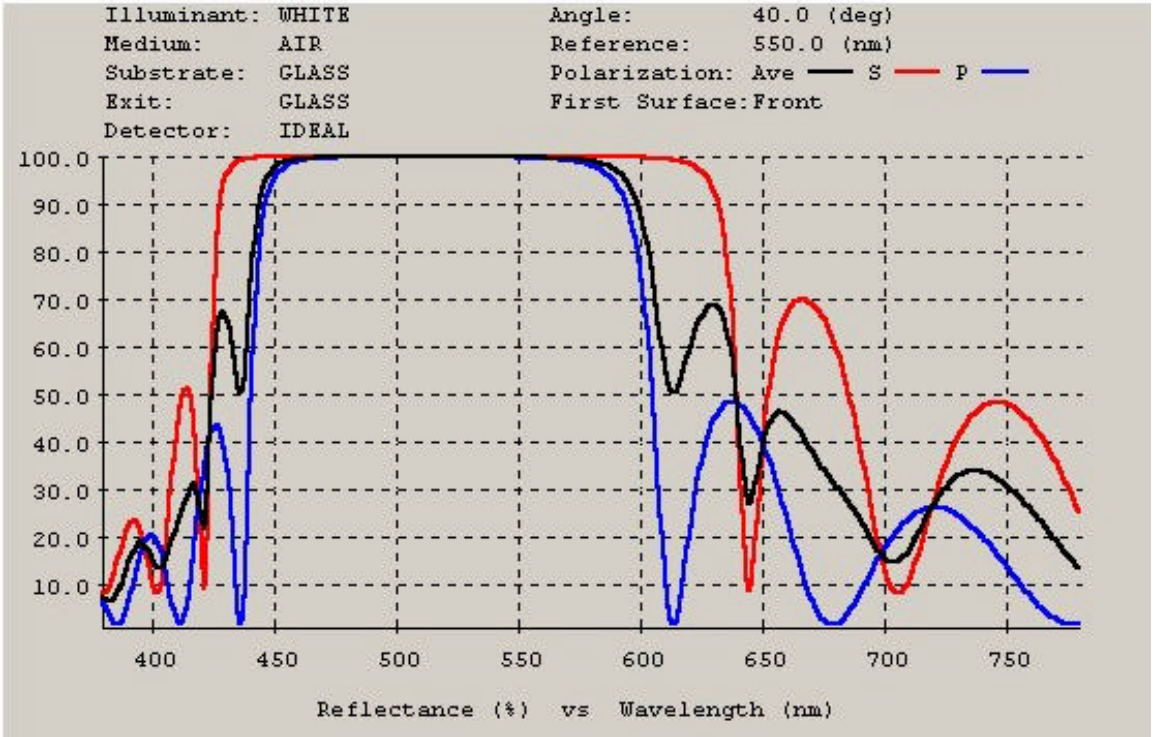

Figure 7-3. Filter response to40^0 incidence.

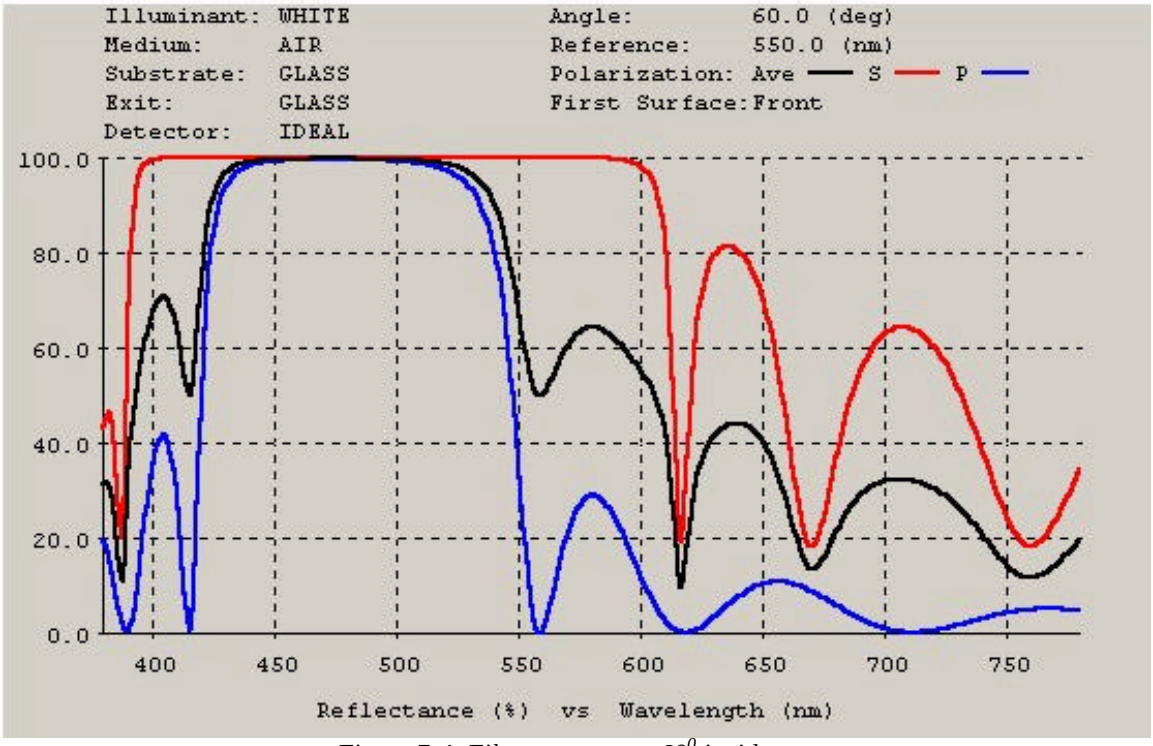

Figure 7-4. Filter response to60^0 incidence.

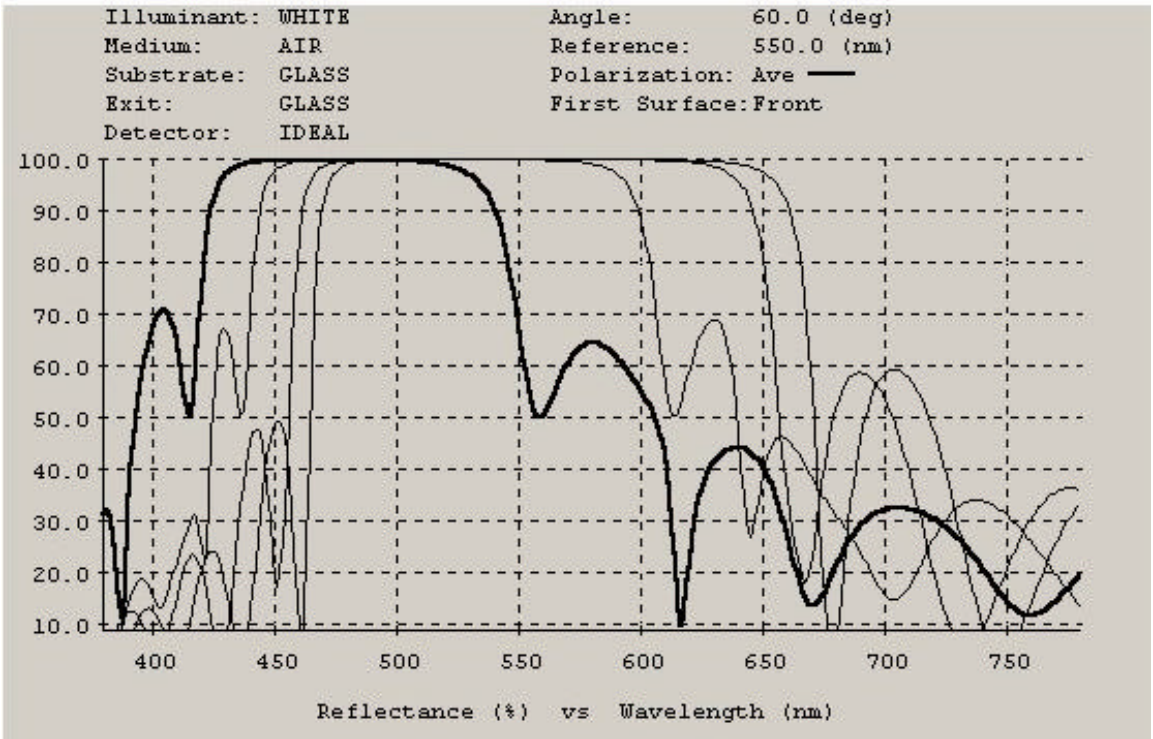

Figure 7-5. Filter response to average polarization at 0^0, 20^0, 40^0,and 60^0 incidence.

From Figure 7-2 to Figure 7-4 the variation in spectral response to different polarization at various incident angles can be understood. Figure 7-5 gives an idea of how the spectral response changes in relation to angle of incident light. Thus it can be seen that incorporating angle of incidence and polarization complicates the analysis, and so in most cases normal incidence and average polarization is assumed.

7.2 Absorbing Media

Till now all the materials considered in the analysis has been considered to be non-absorptive at the operating wavelengths. This is not usually the case. For absorptive media, the refractive index changes from being a real value (n) to a complex value (n-ik). Following the analysis for non-absorbing media, the amplitude reflection coefficients are obtained as before, which holds true for this case also. The analysis becomes complicated and the problem occurs when the analysis is extended to reflectance and transmittance. For the absorbing case, we finally obtain the relation that $1-R \neq T$. This means that the assumption that the intensities can be broken up into separate incident, reflected and transmitted intensities are incorrect and there is a coupling between incident and reflected fields which occur in an absorbing medium.

Although thin film assemblies have absorbing media, the incident media will never be heavily absorbing and so it can be safely assumed to be non-absorbing. As said before the amplitude coefficients for reflection and transmission are valid, and so all calculations of amplitudes in absorbing media will be correct. For calculating the intensities, we have to use,

$R = r.r^*$ and $T = \frac{n_1}{n_0}.t.t^*$ where r and t are the amplitude coefficients of reflection and transmission and r* and t* are its complex conjugates. $N_0 = n_0$ is the refractive index of the incident medium (assumed to be non-absorptive) and $N1 = n_1 - ik_1$ is the refractive index of the second medium.

7.3 Birefringence

Many crystalline substances exhibit optical anisotropy. Their optical properties are not the same in all directions within any given sample. Birefringent materials or crystals are those which display two different indices of refraction. The two indices of refraction are called the ordinary refractive index n_o and the extraordinary refractive index n_e. So a beam of light passing through such a crystal is split into two beams, the ordinary beam and the extraordinary beam. These birefringent crystals have applications in the field of optics.

In recent years research has been underway in the field of fabricating birefringent thin films and their applications. One method of fabricating birefringent thin films is to coat the thin film onto a substrate on which external load has been applied. The load on the substrate is removed after the thin film is deposited. This transfers strain on the substrate to the multilayer coatings. When the isotropic thin film is subjected to stress, it becomes optically anisotropic, due to the photoelastic effect.

Considering one definite thin film structure, let $n_L = n_{Lo}$ and $n_H = n_{Ho}$, be the low and high refractive indices for the ordinary beam and $n_L = n_{Le}$ and $n_H = n_{He}$ be the low and high refractive indices for the extraordinary beam. From these, the phase delay for the ordinary beam, ϕ_o and the phase delay for the extraordinary beam ϕ_e can be calculated. Then the relative phase delay of the birefringent thin film is $\Delta\phi = \phi_e - \phi_o$.

These birefringent films can be used to produce a phase difference between two orthogonal polarization states of the reflected wave. In recent years, efforts have been made to develop birefringent dual-frequency lasers by applying photoelastic effect inside the optical resonators. Using birefringent films, filters having spectral characteristics independent of incident angle or polarization could be designed. This would constitute an interesting area of future work in the thin film filter area.

7.4 Summary

Some factors affecting the spectral response of thin film filters like angle of incidence, polarization, absorption, birefringence etc. have been considered in this chapter.

Chapter 8 Conclusion

The Electrostatic Self Assembly (ESA) process was investigated in depth as a method of making multilayered dielectric spectral filters. The ESA process offers a wide variety of advantages over normal thin film manufacturing methods which makes it extremely suitable for thin film optical coatings. This thesis analyzed the thin film response and performance using TFCalc which is a commercial thin film optical coating design software. Analysis detailing the sensitivity of the coating to manufacturing defects was carried out. This gives a qualitative and quantitative understanding of the sensitivity of the spectral response to layer thickness. The results obtained proved that ESA process, with established upper limits for thickness errors of about 5%, will be an extremely precise method of fabricating these coatings. A thin film filter designed to work at high temperature, blocking out the heat in the radiation emanating from a rocket engine, was designed and analyzed. Some of the factors affecting the spectral response of thin films were also analyzed.

8.1 Future Work

A lot of analysis has been done on thin film optical coatings for the normal incidence, average polarization case throughout this thesis. The performance of thin film filters for varying angles of incidence and different polarizations were also seen. Developing filters whose performance do not depend upon incident angle or polarization could be a very challenging and useful area of future work. Such filters would have the same performance irrespective of the incident light and could be highly useful in different fields where the nature of incident light is not known beforehand, for example in eyeglasses. These kind of filters could be designed by incorporating birefringent materials. Studying the variables involved in the ESA process and developing a stricter control over errors in thickness would also be challenging areas of future work. By improving the process, better, more reliable optical thin films could be fabricated.

REFERENCES

1. H.A. Macleod, *Thin-Film Optical Filters*, McGraw-Hill, New York.
2. A.Thelen, *Design of Optical Interference Coatings*, Mc Graw-Hill, New York (1989).
3. M.Born, E.Wolf, *Principles of Optics*, Pergamon Press, New York.
4. E.Hecht, *Optics*, Addison-Wesley, New York.
5. Y.Liu, A.Wang, R.Claus, "Layer by layer electrostatic self assembly of nanoscale Fe_3O_4 particles and polimide precursor on silicon and silica substrates", *Appl. Phys. Lett.* 71, October 1997.
6. J.D.Hong *et al*, "Layer by layer deposited multilayer assemblies of poly electrolytes and proteins: from ultra thin films to protein arrays", *Progr. Colloid Polym.Sci* 93,98(1993).
7. H.D.Polster, "Reflection from a multilayer filter", *J.Opt.Soc.Am.* 39,12(1949).
8. G.Castagno, F.Demichelis, and E.Minetti-Mezetti, "Design method for multilayer interference filters", *App.Opt.* 19,3(1980).
9. A.Thelen, A.V.Tikhonravov, and M.K. Trubetskov, " Push-button technology in optical coating design: pro et contra", *Part of the Europto Conference on Advances in Optical Interference Coatings, SPIE*, Vol3738.
10. A.V.Tikhonravov, and A.N.Baskakov, "Synthesis of two component optical coatings", Opt.Spectrosc. 56, 915-919 (1984).
11. B.T.Sullivan, J.A.Dobrowolski, "Implementation of a numerical needle method for thin film design", *App.Opt.* 35,28 (1996).
12. TFCalc, Thin Film Design Software for Windows, Version, 3.4.3 manual, Software Spectra, Inc. (1999).
13. Y.Liu, W.Zhao, Y.-X.Wang, and R.O.Claus, "Functionally-tailored nanoparticle-based ionically self-assembled multi-layer thin-films", SPIE , Smart Materials Conference, San Diego (1998).

14. M.Nenkov and T.Pencheva, "Broad band heat reflector design using five layer symmetrical periods from non-absorbing high and low refractive index materials.", *J. Modern Opt.* 45,1,143-152(1998).
15. R.Ulrich, "Interference Filters for the far infrared", *App.Opt.* 7.10 1987-1996(1968).
16. K.F. Renk and L.Genzel, "Interference Filters and Fabry-Perot Interferometers for the far infrared", *App.Opt.*1,5 643-648(1962).
17. W.Mao, D.Lin, C.Yin, Y.Huo, "Bireflectance thin film in a high beat frequency laser", *Opt. & Laser Tech.*, 33, 341-345(2001).
18. C.Caliendo, E.Verona, G.Saggio, "An integrated optical method for measuring the thickness and refractive index of birefringent thin films", *Thin Solid Films*, 292, 255-259 (1997).
19. Y. Liu, A. Wang and R.O. Claus, "Molecular Self-Assembly of TiO_2/Polymer Nanocomposite Films," *J. Phys. Chem.* B 1997, 101, 1385-1388.
20. F.J. Arregui, Y. Liu, I.R. Matias, R.O. Claus, " Optical Fiber humidity Sensor Using a Nano Fabry-Perot Cavity Formed by the Ionic Self-Assembly Method", *Sensors and Actuators* B 3000, 1999.
21. Y. Liu, Y.-X. Wang, H. Lu and R.O. Claus, "Electrostatic Self-Assembly of Highly-Uniform Micrometer-Thick Fullerene Films", *J. Phys. Chem* B. 1999, 103, 2035.
22. W. Zhao, J. Wang, A. Wang and R. Claus, "Geometric analysis of optical fiber EFPI sensor performance", *Smart Materials and Structures* 7 (1998), p. 907-910.
23. . Zhang, F. Zhang, K. Cooper, Y. Wang, Y.Liu and R.O. Claus, "Electro-Optic Property Measurement of Electrostatically Self-Assembled Ultrathin Films", *Optics Communications*, Article 7034, Pg 01-7, November 2000.
24. Y. Liu, A. Wang and R.O. Claus, "Ionic Self-Assembled Monolayer Multi-Layer Thin-Films" , SPIE Smart Structures & Materials, San Diego, CA., Feb 1997.
25. Y. Liu, A. Rosidian, K. Lenahan, Y-X. Wang, T. Zeng and R. Claus, "Characterization of electrostatically self-assembled nanocomposite thin films", *Smart Materials and Structures* 8 (1999), p. 100-105.

VITAE

ASHWIN CHANDRAN

Ashwin Chandran was born in Kerala, India on February 26 1977. After receiving the Bachelor of Technology in Electrical Engineering from Kerala University, India in October 1998, he worked as a software engineer with Infosys Technologies Ltd, India from 1999 to 2000. He then went on to Complete his Master of Science in Electrical Engineering from Virginia Polytechnic and State University in September 2001 and is currently pursuing a PhD in Electrical Engineering. Has been working as a Graduate Research Assistant at the Fiber and Electro-Optic Center at Virginia Polytechnic and State University since May 2001.